NAVAL POSTGRADUATE SCHOOL

MONTEREY, CALIFORNIA

THESIS

WIRELESSLY NETWORKED DIGITAL PHASED ARRAY: ANALYSIS AND DEVELOPMENT OF A PHASE SYNCHRONIZATION CONCEPT

by

Micael Grahn

September 2007

Thesis Advisor:	David Jenn
Second Reader:	Robert Broadston

Approved for public release; distribution is unlimited

THIS PAGE INTENTIONALLY LEFT BLANK

REPORT DOCUMENTATION PAGE		Form Approved OMB No. 0704-0188

1. AGENCY USE ONLY *(Leave blank)*	2. REPORT DATE September 2007	3. REPORT TYPE AND DATES COVERED Master's Thesis

4. TITLE AND SUBTITLE Wirelessly Networked Digital Phased Array: Analysis and Development of a Phase Synchronization Concept	5. FUNDING NUMBERS
6. AUTHOR(S) Micael Grahn	
7. PERFORMING ORGANIZATION NAME(S) AND ADDRESS(ES) Naval Postgraduate School Monterey, CA 93943-5000	8. PERFORMING ORGANIZATION REPORT NUMBER
9. SPONSORING /MONITORING AGENCY NAME(S) AND ADDRESS(ES) Office of Naval Research Arlington, Virginia	10. SPONSORING/MONITORING AGENCY REPORT NUMBER

11. SUPPLEMENTARY NOTES The views expressed in this thesis are those of the author and do not reflect the official policy or position of the Department of Defense or the U.S. Government.

12a. DISTRIBUTION / AVAILABILITY STATEMENT Approved for public release; distribution is unlimited	12b. DISTRIBUTION CODE

13. ABSTRACT (maximum 200 words)

The ongoing research of a wirelessly networked aperstructure digital phased array (WNADPA) at NPS has investigated the possibility of using a distributed opportunistic array for radar, where array elements are placed at any available area of the ship structure. This could give an array that is as large as the ship itself, with 360 degrees coverage. It has advantages in the areas of survivability and adaptability, and the profile of the ship could be kept low for better maneuverability and smaller radar cross section.

The array elements are stand-alone transmit-receive (T/R) modules controlled over a wireless media, with no hardwire connection other than power supply. Phase and time synchronization are critical for the successful operation of the array. The focus of this thesis is on designing a phase synchronization concept, implementing it in existing T/R modules using Commercial of the Shelf (COTS) hardware, and performing validation measurements of the proposed phase synchronization process. The results verify that distribution and phase synchronization of a local oscillator signal over the free space channel are possible.

14. SUBJECT TERMS Phased Array, Phase Synchronization, Aperstructure, Radar, Modulator, Demodulator, Transmit/ Receive module, Digital beamforming, Demonstration Array.	15. NUMBER OF PAGES 88
	16. PRICE CODE

17. SECURITY CLASSIFICATION OF REPORT	18. SECURITY CLASSIFICATION OF THIS PAGE	19. SECURITY CLASSIFICATION OF ABSTRACT	20. LIMITATION OF ABSTRACT
Unclassified	Unclassified	Unclassified	UU

NSN 7540-01-280-5500

Standard Form 298 (Rev. 2-89)
Prescribed by ANSI Std. 239-18

THIS PAGE INTENTIONALLY LEFT BLANK

Approved for public release; distribution is unlimited

WIRELESSLY NETWORKED DIGITAL PHASED ARRAY: ANALYSIS AND DEVELOPMENT OF A PHASE SYNCHRONIZATION CONCEPT

Micael J. Grahn
Lieutenant Colonel, Swedish Armed Forces (Army)
B.S., Swedish National Defence College, 2004

Submitted in partial fulfillment of the
requirements for the degree of

MASTER OF SCIENCE IN ELECTRONIC WARFARE SYSTEMS ENGINEERING

from the

NAVAL POSTGRADUATE SCHOOL
September 2007

Author: Micael Grahn

Approved by: David Jenn
Thesis Advisor

Robert Broadston
Second Reader

Dan Boger
Chairman, Information Sciences Department

THIS PAGE INTENTIONALLY LEFT BLANK

ABSTRACT

The ongoing research of a wirelessly networked aperstructure digital phased array (WNADPA) at NPS has investigated the possibility of using a distributed opportunistic array for radar, where array elements are placed at any available area of the ship structure. This could give an array that is as large as the ship itself, with 360 degrees coverage. It has advantages in the areas of survivability and adaptability, and the profile of the ship could be kept low for better maneuverability and smaller radar cross section.

The array elements are stand-alone transmit-receive (T/R) modules controlled over a wireless media, with no hardwire connection other than power supply. Phase and time synchronization are critical for the successful operation of the array. The focus of this thesis is on designing a phase synchronization concept, implementing it in existing T/R modules using Commercial of the Shelf (COTS) hardware, and performing validation measurements of the proposed phase synchronization process. The results verify that distribution and phase synchronization of a local oscillator signal over the free space channel are possible.

THIS PAGE INTENTIONALLY LEFT BLANK

TABLE OF CONTENTS

LIST OF FIGURES

LIST OF TABLES

THIS PAGE INTENTIONALLY LEFT BLANK

ACKNOWLEDGMENTS

I want to express my gratitude to Professor David C. Jenn for his huge support and expert guidance throughout this work. His door has always been open, and throughout all the discussions we have had, he's provided invaluable help for my work.

Special thanks also go to Mr. Robert D. Broadston, Microwave Lab Director, for always providing me with enthusiastic solutions to whatever question I had regarding my work.

Finally, I would like to thank my wife AnnaKarin and our two children Nils and Anna for all the cheering and support they have provided during this time.

THIS PAGE INTENTIONALLY LEFT BLANK

I. INTRODUCTION

A. BACKGROUND

The World is facing a more global threat when new states are continuously announcing their capability of launching nuclear ballistic missiles. The United States is therefore fielding a Ballistic Missile Defense System (BMDS) to provide protection against such threats. The BMDS is a system that includes target detection in all phases of the missile trajectory which means that the sensor systems that are used to detect the missile need to be deployed globally. Figure 1 shows the BMDS concept where phased array antennas are playing a vital role as sensors and part of the interceptor controls.

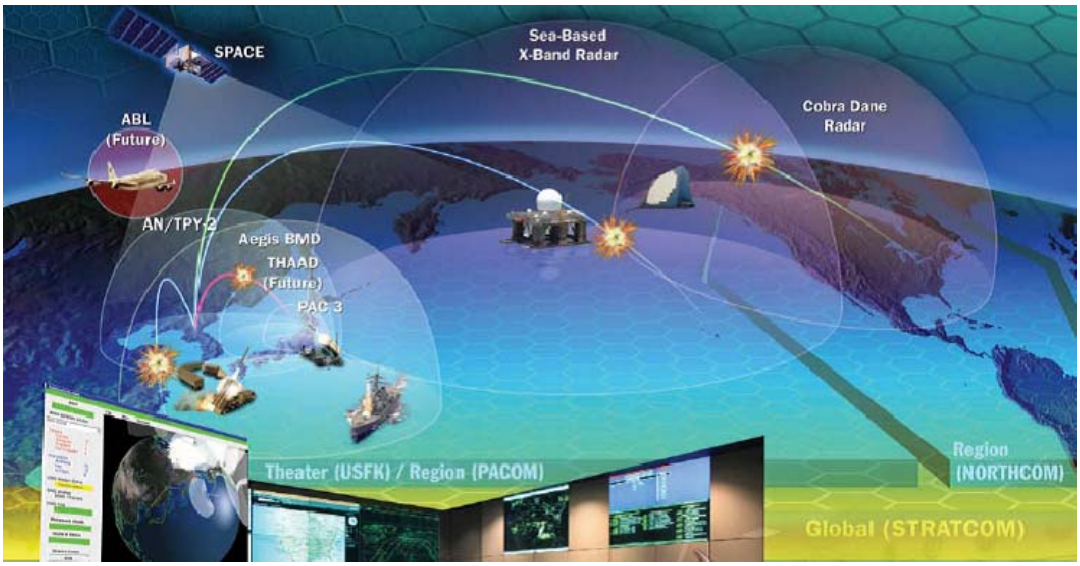

Figure 1. BMDS Concept (From [1]).

The BMDS uses a variety of sensors like Cobra Dane radar, Sea-Based X-Band radar, Forward-Based AN/TPY-2 radar, and the AN/SPY-1. Most of these radars use phased array antennas that are deployed strategically and linked together through a Command and Control system to give a global coverage and early warning. Cobra Dane

and AN/TPY-2 (see Figure 2) use heavy and large phased array antennas, designed to be at fixed ground positions. They are not suitable for mounting on a ship, unlike the AN/SPY -1.

Figure 2. Cobra Dane and AN/TPY-2 (From [2]).

The Aegis BMD uses AN/SPY-1 which is a multifunction phased array radar system that uses frequencies in the S-band, and can track up to 100 targets in any direction, at any given time [3]. The radar panels have been mounted directly on the ship's superstructure using flat panels. The four panels give a 360 degree radar coverage. Figure 3 shows these panels mounted on USS Lake Erie.

Figure 3. Cobra Dane and AN/TPY-2 (From [4]).

The AN/SPY-1 radar has a high peak power of 4 MW, but together with a low antenna height the system only gives an estimated detection range of 200 nm [3]. This range is not sufficient for a BMD Early Warning Radar (EWR) system for rapid and forward deployment with great range coverage. To meet the higher demands for range coverage together with the resolution needed for missile guidance, the next generation of destroyers for the US Navy, the Zumwalt-class DDG 1000, are equipped with Dual Band Radar (DBR).

The radar for the weapon system and missile guidance uses the X-band, and the EWR uses the L-band. The AN/SPY-3 Multi Function Radar (MFR) is the X-band active phased-array radar that will take care of the short range high resolution requirements, while the L-band Digital Array Radar (DAR) will be used as the Volume Search Radar (VSR) for DDG 1000, see Figure 4. The L-band DAR fully digitized T/R modules, connected with fiber optics in a novel antenna architecture, complements the AN/SPY-3 radar and gives the DDG 1000 a far better range detection and EWR capability [5].

Figure 4. DDG 1000 (From [6]).

Even if dual band radars can complement each other and give both range and high resolution, the angular resolution is still dependent on the size of the aperture, which should be as large as possible. Unfortunately, the aperture is limited so as to fit into the ship architecture without affecting maneuverability and radar cross section (RCS).

So how can we have a large aperture without affecting these parameters? A possible solution to this problem could be the wirelessly networked aperstructure digital phased array (WNADPA) research at NPS. The research examines the possibility of integrating distributed T/R elements into the platform structure, which could give an aperture the size of the platform. In the DDG 1000 case, the aperture size would be about 600 ft. If this entire length is available to a radar that is using the UHF band, the combined performance and range detection would be noticeably increased.

B. PREVIOUS WORK

The WNADPA has been an ongoing project at NPS for four years, and several students contributed to its current status. The previous work is presented below.

Tong [7] examined the detection range for a DD(X)-sized ship. He built a CAD model of the ship, and distributed various numbers of antennas all over the ship structure. Then he used a MATLAB program to plot the beam pattern and the main lobe gain. These data were then used to plot the performance versus the number of elements used in the array. Approximately 400 elements were needed to achieve a detection range of 1000 km. He also designed and simulated a U-slot antenna, and verified its electrical characteristics.

Yong [8] verified the linear relationship between the modulator board and the demodulator. He used an AD8346 as a transmitter, and swept its output phase over 360 degrees. He connected AD8346 output to AD8347 input, and took notes on the I/Q average voltage levels. The result showed a linear relation between transmitted phase and measured phase. He also investigated the possibility of distributing the LO and Data signals to the antenna element over wireless media, and the results showed that this was possible.

Loke [9] examined two different methods of wireless synchronization for the T/R modules. The “brute force” synchronization technique that synchronizes each element in turn, was slow, but simple and easily implemented in hardware. He also examined the

hull's dynamic deflections, and their impact on the array element positions. His conclusion was that no motion correction was needed for a system operating in the VHF/UHF frequency bands.

Burgstaller [10] did a characterization of all the hardware contained in a T/R module. Transmission loss, isolation, gain, attenuation and standing wave ratio (SWR) where measured and verified against different vendors' specifications. The hardware was then integrated into a demonstration T/R module. He also modeled a proposed eight-element linear array in both MATLAB and CST Microwave studio.

Yeo [11] worked together with Burgstaller to develop the two T/R modules, and all the connection cables that where needed for the demonstration setup. He also designed a user interface in LabVIEW to control and verify the demonstration setup. Several measurements where conducted to characterize and verify the T/R module performance. One of the measurements was to observe the occurrence of interference between the modulator and demodulator during operation, and the result was that no observable interference occurred.

Under recommendations for future work by previous researchers [7-11], is the need for a phase synchronization concept and a circuit to implement that concept into existing T/R modules. There have been several proposals and suggested solutions, but so far no verified solution or hardware implementation.

C. STATEMENT OF PROBLEM

This thesis continues the work with WNADPA, which has been an ongoing research project at NPS for the past four years. Several students have been involved, and a demonstration array of two T/R-elements has been developed. Until now the phase synchronization process has only been a theoretical black box, and since this process is vital for the continuing work, a hardware concept and its development was necessary.

The focus of this thesis will be on designing a phase synchronization concept, implement it in existing T/R modules using Commercial of the Shelf (COTS) hardware, and perform validation measurement of the proposed phase synchronization process.

D. ORGANIZATION OF THE THESIS

Chapter I has presented a short background and motivation for the WNADPA project. Chapter II gives an overview of the radar concept and how it can be applied to a ship structure. Chapter III starts with a system analysis of the whole WNADPA concept, to get a good basis for understanding tradeoffs and requirements. The design section discusses and analyzes the concept for the phase synchronization.

Chapter IV analyzes the device parameters such as transmission loss, isolation and reflection for the new hardware that will form the synchronization unit. Then measurements are shown for a prototype phase synchronization system setup, to verify the theoretical concept. Finally a full implementation is added to the T/R modules. Chapter V is where the concept is verified through a series of measurements. Chapter VI summarizes the thesis with conclusions, and gives recommendation for further and future research.

II. ARRAY SYSTEM ARCHITECTURE

A. BACKGROUND

This chapter summarizes the WNADPA research at NPS: what previous students have done in the past, where we are right now and what the long term goals are. It provides an overview of the whole concept and how it can be applied on a ship structure.

Phased array radar systems are commonly used by warships all around the world. There has always been a challenge to construct a radar system that meets all requirements. One important parameter is angular resolution, which increases with antenna aperture. Large antenna arrays can be a solution for ground based systems, but not on a warship where low weight, low profile and low RCS are important. Large antennas are also difficult to maintain and their weight can affect the maneuverability of the ship.

The WNADPA research at NPS looks at the possibility of using an opportunistic array where array elements are distributed over available areas of the ship structure. This could give an array that is as large as the platform itself, with 360 degrees coverage, and the profile of the ship could be kept low for better maneuverability and smaller RCS.

B. ARRAY ARCHITECTURE

1. Overview

The array consists of small antennas and T/R-modules placed at various areas of the ship. The antenna elements are preferably integrated into the hull structure, with only the antenna element facing the outside. They are controlled over wireless media from a Controller, with no need for a wire connection, except for a power supply (see Figure 5). The number of elements used depends on the platform structure, and the purpose of the radar system.

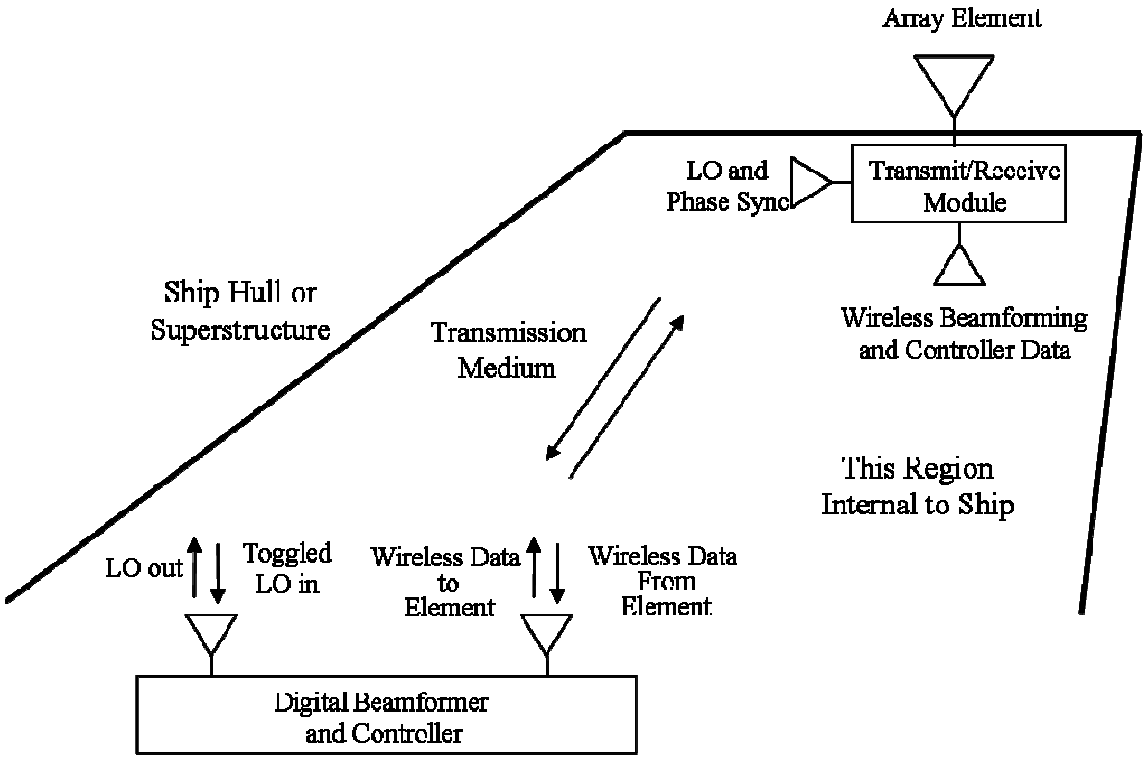

Figure 5. Array system overview (From [12]).

If the elements could be distributed and integrated into the superstructure of the platform, their exposure to external threats would dramatically decrease. Contaminants like dirt, water, or even fragments from a shell fire detonation could be avoided. But more important the platform could keep a stealthy shape and increase its overall survivability. To achieve this, the elements need to be an integral part of the hull production from the early design phase, as depicted in Figure 6. The figure also shows an integrated transmission system for sending data between the elements and the Controller. Free space wireless links through the ship spaces are another approach that is discussed.

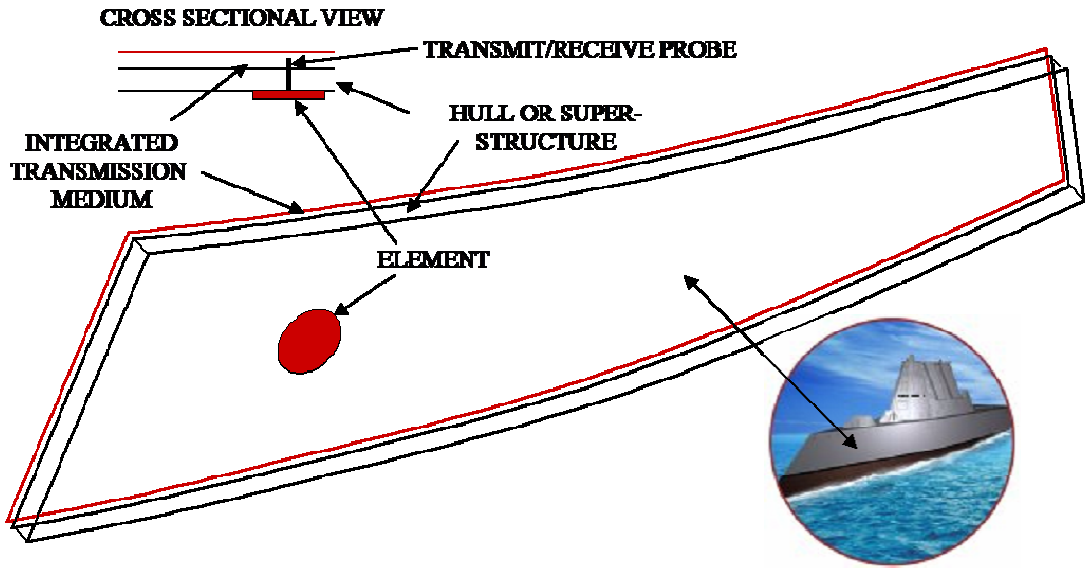

Figure 6. Integrated transmission medium (From [8]).

The only part that needs to be in contact with the transmission medium is the transmit/receive module, which in turn connects to an array antenna element. A 300 MHz u-slot antenna, shown in Figure 7, is a candidate for integration into the ship structure. In addition, the T/R modules have antennas for the internal wireless network and local oscillator (LO) distribution.

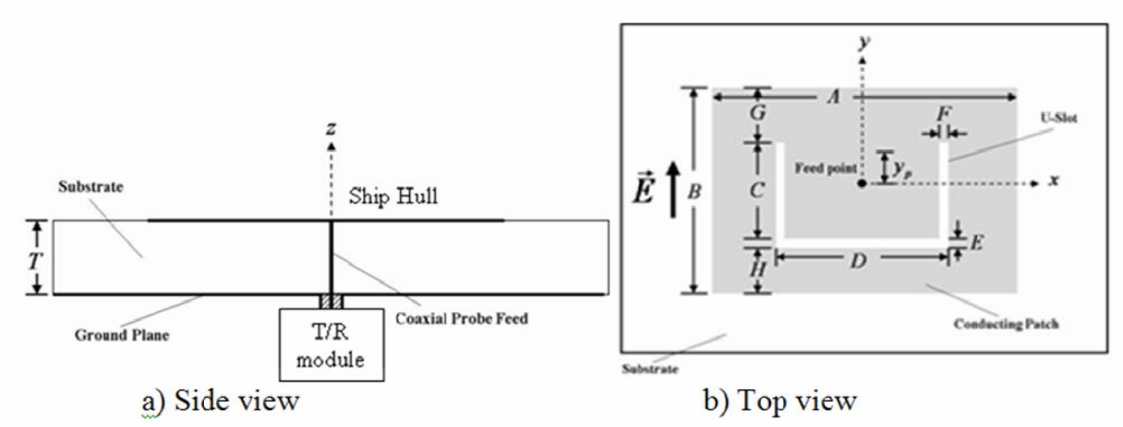

Figure 7. U-slot antenna (From [12]).

2. Wireless Network

Since the concept could involve thousands of distributed elements all over the platform, a wired solution to every element would be very difficult to manage. The T/R-modules are therefore controlled wirelessly from a Controller and beamformer. Beamforming control signals manage the phased array operation, while the timing signals take care of the LO distribution and phase synchronization.

The data throughput necessary for radar processing will be demanding and the available COTS systems on the market today can barely handle it. But the growing market for small office and home office networks (SOHO), have put a pressure on the wireless industry. New and faster systems are introduced every 6 months, and advances in wireless communication will make the WNADPA concept realizable in the near future. The wireless network challenges are being addressed in a related thesis [13].

3. Demonstration T/R Module

The T/R module is the self standing unit that will form an array element in the phased array structure. Each module will have a small RF antenna integrated in the platform structure. The goal is to communicate wirelessly to each module from the Controller. A fully functional demonstration array was developed using COTS components at 2.4 GHz. A block diagram of the demonstration module without the synchronization circuit is shown in Figure 8.

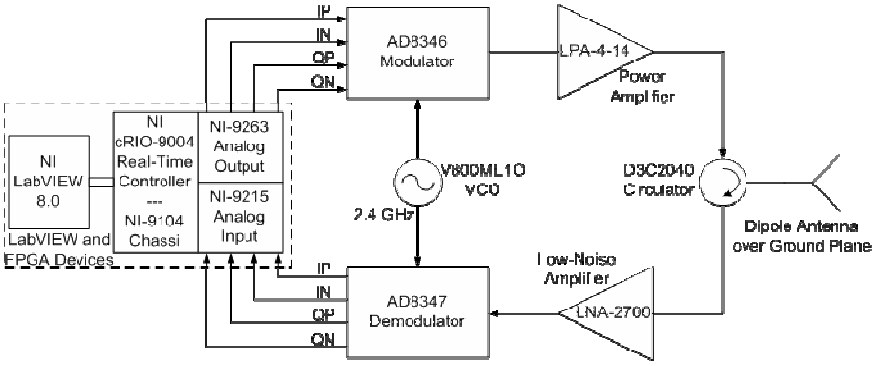

Figure 8. Simplified T/R module using hard–wired LO signal (From [10]).

The module has a basic radio layout with separate receive and transmit parts. The receiving part consists of a low-noise amplifier and a demodulator, while the transmit part has a modulator and a power amplifier. The module uses one antenna and a circulator for separating transmit and receive signals. For the demonstration setup, the array element output is hardwire-connected between the two modules using a coaxial cable as shown in Figure 9.

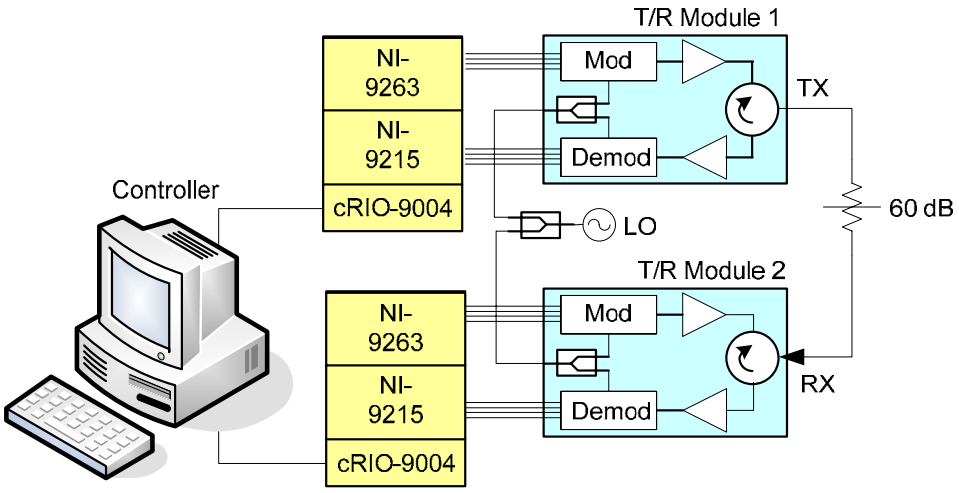

Figure 9. Two element demonstration setup using a cable and attenuator in place of the free space channel.

4. Controller

a. Controller and Processor

The central processor is where the phased array antenna is controlled and all the data from and to the elements is processed. For the demonstration array the Controller consists of a central computer, software and Field Programmable Gate Arrays (FPGAs). The software and hardware used to handle this function for the demonstration setup is from National Instruments (NI) (see Figure 10).

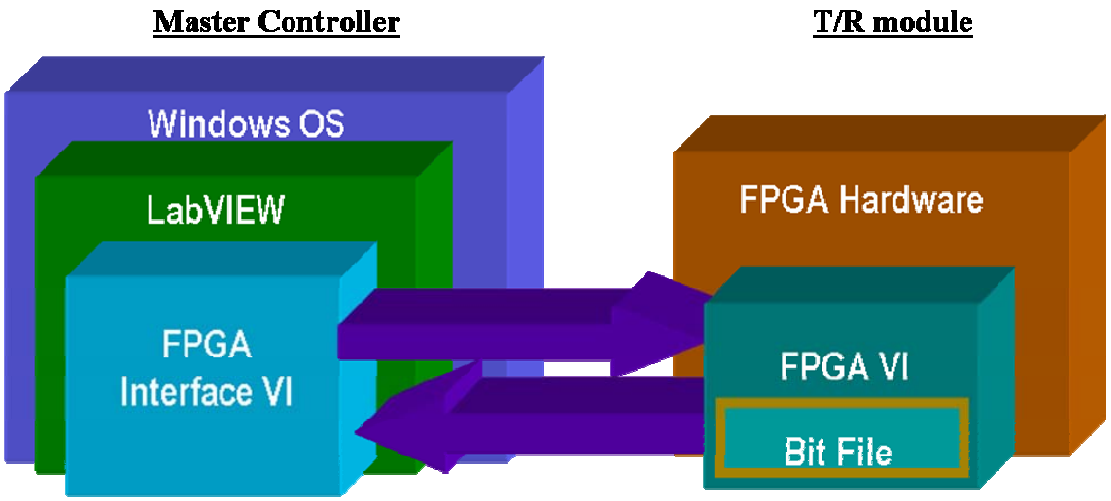

Figure 10. Schematic model of the LabVIEW Software interface (From [10]).

b. LabVIEW

The software chosen for the demonstration is LabVIEW from NI. This is a graphical development platform, where program can be developed directly from the user interface using virtual instruments or VIs. An example of a control panel comprised of LabVIEW defined functions is shown in Figure 11.

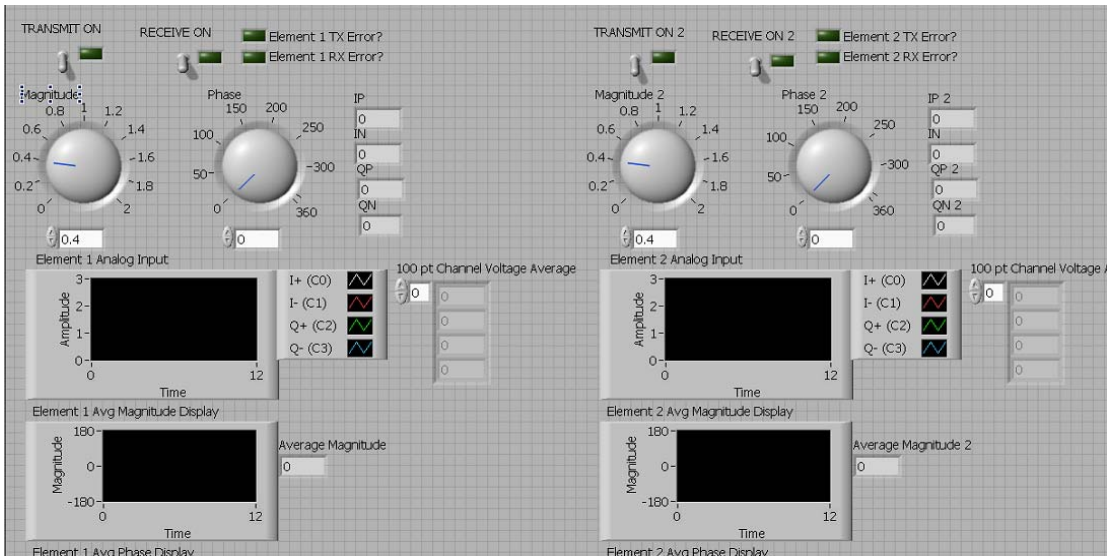

Figure 11. LabVIEW user interface (From [11]).

c. FPGA

The demonstration setup uses NI LabVIEW FPGA software to create custom applications for hardware. The Controller, chassis, analog output module (D/A), and analog input module (A/D) are shown in Figure 12. The programming takes place in LabVIEW using a block diagram constructed with the FPGA virtual instrument (VI). When the programming is done, it is compiled and downloaded to a reconfigurable I/O (RIO) device. This means that it is fairly simple to add extra functions, or to modify applications, without changing the hardware.

Figure 12. NI cRIO system (From [14-17]).

The Controller interfaces with the modulator and demodulator as shown in Figure 13. Baseband in phase (I) and quadrature (Q) voltages are passed between the Controller and the RF section. The Controller is a standard windows based PC with LabVIEW software, and it communicates with the FPGA through its network card, and a standard unshielded twisted pair (UTP) cable.

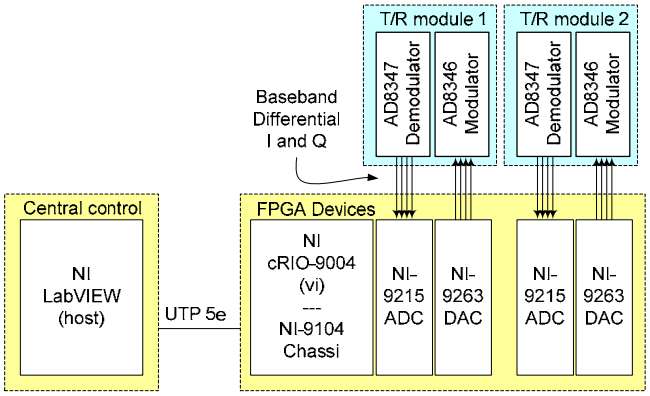

Figure 13. NI cRIO demonstration setup.

C. PHASE SYNCHRONIZATION

A phased array antenna is a group of antennas where the radiation pattern is controlled by changing the individual element phases. The phase change is relative, and a system needs a common phase reference. This common reference is necessary to scan the beam and control the radiation pattern. Every element needs an accurate phase reference for the mixing process (i.e., local oscillator, LO) and the Controller needs to know every element's location relative the reference, so that this difference can be added in the software for beamforming and control of the radiation pattern. For the WNADPA the LO signal will be transmitted wirelessly as a beacon. Since this relative phase could change over time due to reflection and multi-path transmission, the phase synchronization process needs to be performed periodically in the background.

Earlier research has examined different techniques for synchronization. Loke [9] tried a brute force approach, which showed good results. The concept needs a small amount of hardware implemented in each module as shown in Figure 14, labeled as the "Sync Circuit". One element is chosen as the reference (master), and all the rest (slaves) synchronize their phase to this reference element.

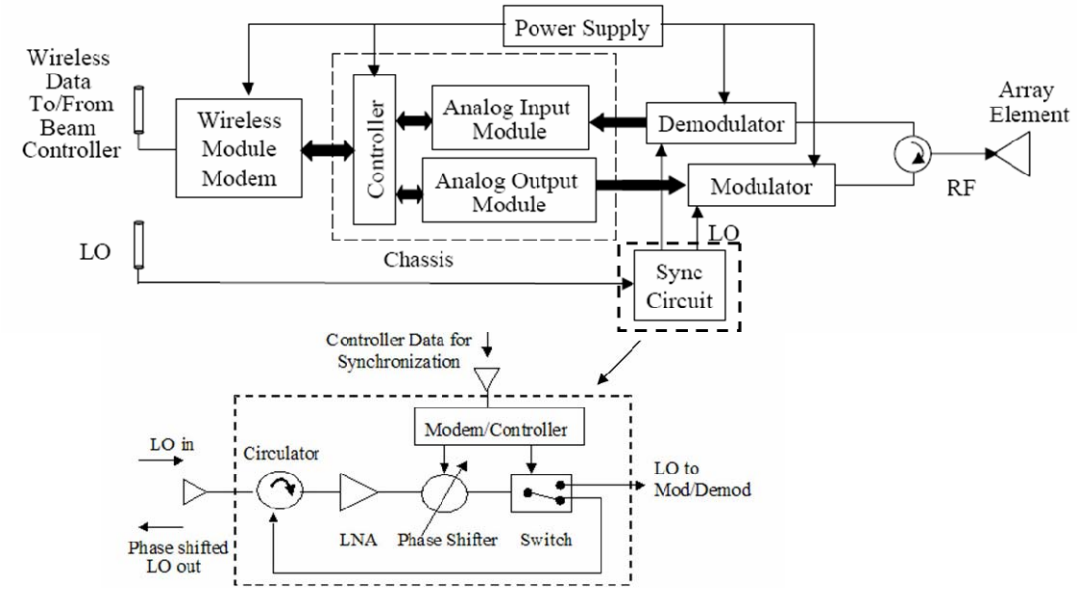

Figure 14. Diagram of possible sync circuit in T/R module (From [9]).

The brute force concept only allows one element at a time to be synchronized, so when the first element is chosen, it goes into a synchronization mode. This is done by a switch that, in sync mode, returns the LO signal back to the Controller for comparison with the returned reference LO as shown in Figure 15. The comparison algorithm subtracts the two signals in a detector and looks at the resulting voltage level, and then sends controller data to the element, telling it to step up the phase one step. The element sends the LO back for a new comparison, and the new voltage level is compared to the previous one. If the level is decreasing, a new up shift is sent; if it is increasing a down shift is sent. This continues until the algorithm finds the lowest voltage level, and thus its relative phase shift for that particular element. This phase is stored in the Controller software. This procedure is then repeated for every element in the array. Although this technique is inefficient with regard to convergence, it is acceptable for the WNADPA. A phase accuracy of 20 degrees is sufficient, so not many phase steps have to be taken to reach a minimum, especially if the channel is only slowly varying.

The comparison algorithm is looking for the minimum voltage level after the two signals are subtracted. That minimum occurs when the reference element and the element in synchronization have their LO, back at the Controller, 180 degrees apart. If their amplitudes are equal, the level should be zero, but in a real and continuously changing environment equal amplitudes are not likely. However, the subtraction still gives a notch deep enough to determine the phase correction.

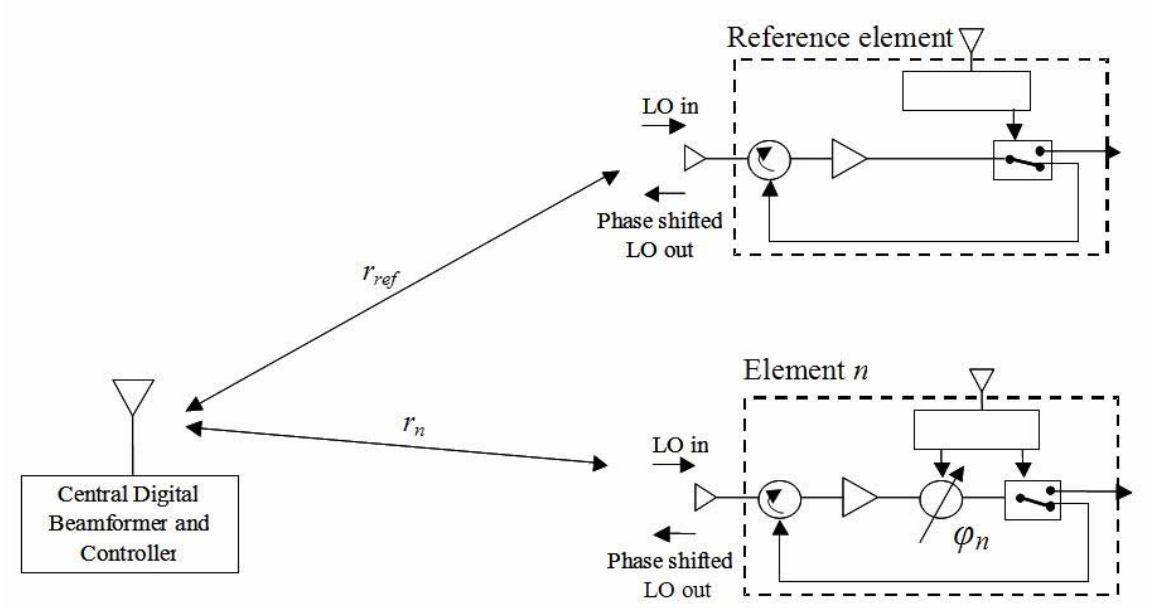

Figure 15. LO phase synchronization concept (From [9]).

D. SUMMARY

This chapter has provided an overview of the whole distributed array concept and how it can be applied on a ship structure. It also addressed some of the basic hardware issues. The next chapter describes the demonstration array and measurements conducted to validate the synchronization hardware.

III. DEMONSTRATION ARRAY DESIGN

A. BACKGROUND

A phased array antenna needs to have each element synchronized in phase for coherent operation and the ability to scan the beam. This is relatively easy if you have the elements wired to a common frequency reference, but in the WNADPA we propose to have the elements receive the frequency reference wirelessly from a common source. For the conventional wired solution there is a stable propagation path, with a fixed and known distance. The wired distance is known precisely through calibration and the processor knows each element's relative phase.

In the WNADPA each element is wirelessly connected so the phase synchronization is a challenge. There is a need for a wireless phase synchronization design, verification and implementation. There have been a number of good algorithms proposed and simulated, but so far no hardware implementation. The simplest solution is the "brute force" technique proposed by Loke [9]. It is the easiest to implement in hardware and the one selected for the demonstration array.

This chapter examines the different parts of the demonstration setup and in particular the part that performs phase synchronization. The basic parts of the demonstration array are shown in Figure 16. It is comprised of a Controller and processor and two T/R modules with antenna elements. One element is a reference and the other a slave to be synchronized. Each demodulator needs to be calibrated before installation into the module. A brief description on how to do the demodulator calibration is therefore part of this Chapter. For the synchronization process, the demodulator is switched out and not in operation.

For data communication there is a wireless network connecting the two elements to the Controller. The user interface and system control software is written in LabVIEW. In the next section the various components of the demonstration array and their functions are described.

B. WIRELESS NETWORK

The data and control communication between the Controller and the elements is achieved using a commercial wireless local area network (WLAN). We also need to provide an LO signal for the demodulator and modulator boards. The LO is then fed back to the Controller for phase measurement in the sync mode. The LO frequency is set by the operating frequency of the radar (2.4 GHz). The data WLAN should be on a separate frequency to avoid interference with the LO signal. Since this is a demonstration setup where we use COTS, the two available bands for SOHO wireless networks are 2.4 GHz and 5.8 GHz. Since the LO frequency is set to be 2.4 GHz, we need to have the data channel on 5.8 GHz.

The normal wireless setup is to have a master and slave configuration. An access point is therefore connected to the Controller, and it controls the communication with the elements. The standard chosen for this is 802.11a, which operates in the 5.8 GHz band.

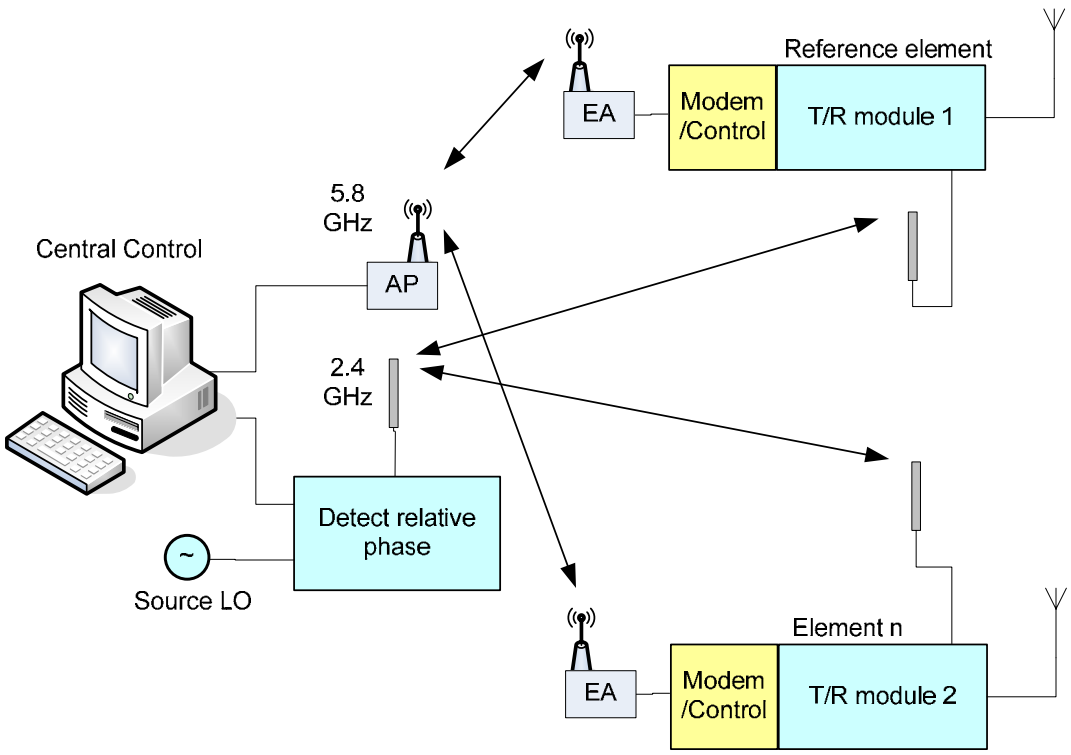

Figure 16. Demonstration array configuration.

C. CONTROLLER

The Controller sends transmit waveform data, collects received data and performs synchronization and timing. It also does the beamforming and radar processing. The Controller needs to know every element's relative phase to a common reference. The phase differences are then used as an input to the beamforming to compensate for the differences in path length between elements.

The Controller is a standard Windows-based computer with serial and parallel ports. These ports can not directly read RF, nor can they read an analog voltage level. First the signals must be passed through an ADC. This can be done with a voltage meter with a digital output. The digital voltage level is then fed to the parallel port, and made available for the program to read. Each voltage level is compared to the previous measurement and then the Controller sends an up or a down phase-shift command to the element that is currently under synchronization until a minimum is reached.

For synchronization the T/R module must contain hardware capable of changing between synchronization and normal modes, as commanded from the Controller. This could be done with a TTL controlled switch, connected to a LabVIEW FPGA digital output in the T/R module as seen in Figure 17.

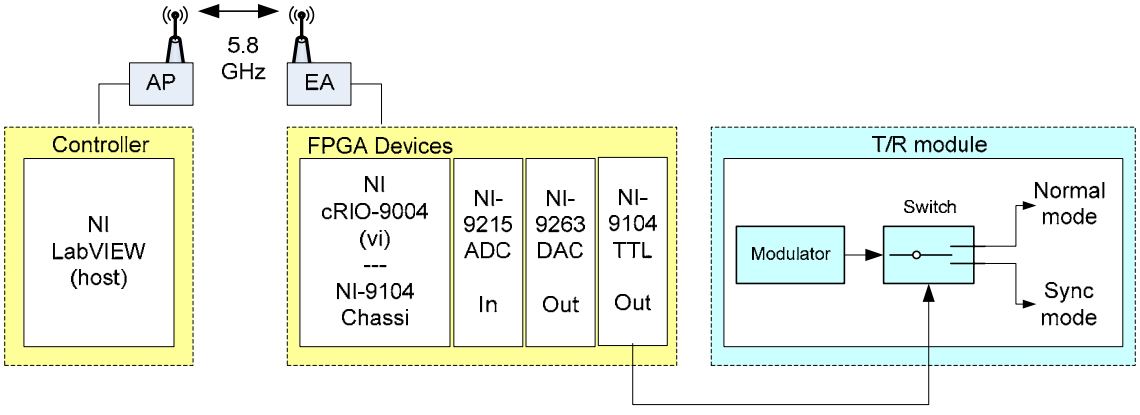

Figure 17. NI Hardware for validating the synchronization mode control.

D. T/R MODULE

1. Modulator

A T/R module design based on COTS hardware was proposed by Burgstaller [10] and built by Yeo [11] as shown in Figure 18. However the modules did not have a synchronization circuit included. The original synchronization algorithm proposed by Loke requires some type of phase shifting device in the module so that the reference signal can be phase shifted and returned to the Controller.

The AD8346 modulator from Analog Devices [18-20] is the vital part of the transmit chain in the T/R module. The modulator is also a possible phase shifter in the phase synchronization process. If it is possible to use this device as a phase shifter in the sync mode, instead of a separate phase shifter device, we could reduce the size and cost of the T/R modules.

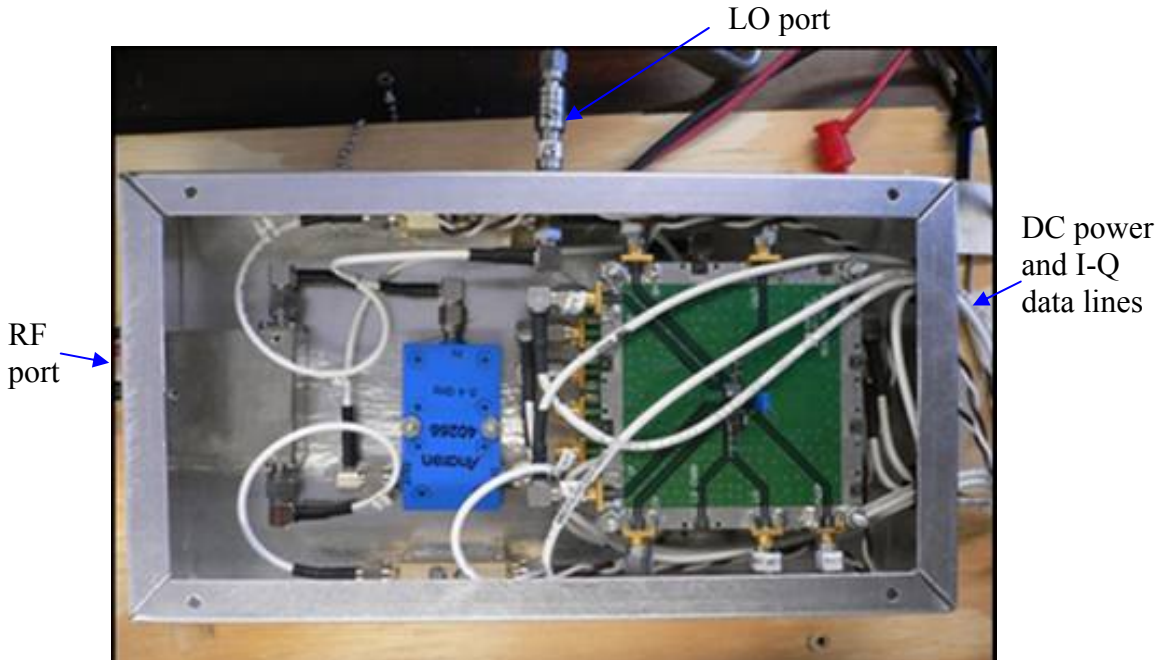

Figure 18. Assembled T/R module (From [11]).

Since the T/R module in synchronization mode is not using its modulator, it is possible to use it as a phase shifter. A measurement was performed to verify its relation between the input voltages on I/Q and their output phase shift. The connection from the Controller to the modulator input is already established, so the only modification is to have its output switching between the sync mode and normal mode as shown in Figure 17.

The test setup to verify the modulator performance in the new sync circuit is shown in Figure 19. To get the proper levels on the input, which translates to the desired phase output, LabVIEW is used. The VNA provided the LO on port 1, and measured the phase shift on port 2.

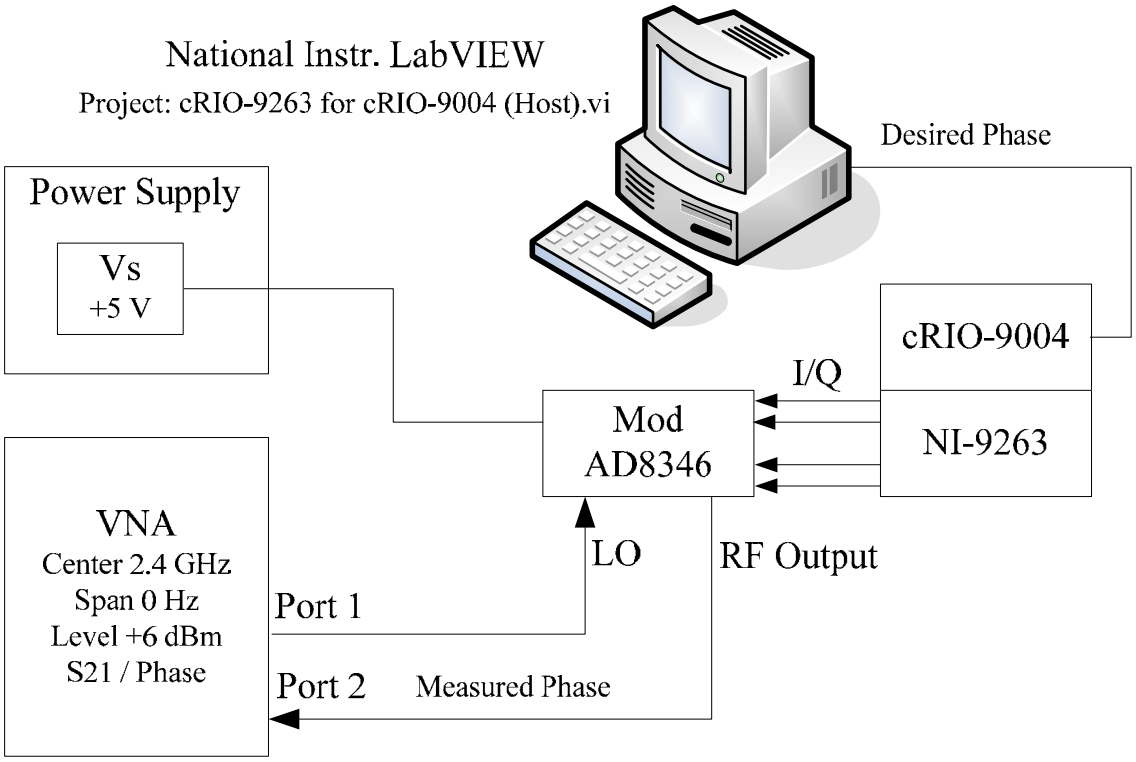

Figure 19. AD8346 phase measurements setup to validate its use in the sync circuit.

The measurement was done over a range of 360 degrees where the phase is measured every 10 degrees. The plot in Figure 20 shows a phase error span of six degrees over the 360 degrees, with the maximum error on the I and Q axes (0º, 90º, 180º, 270º).

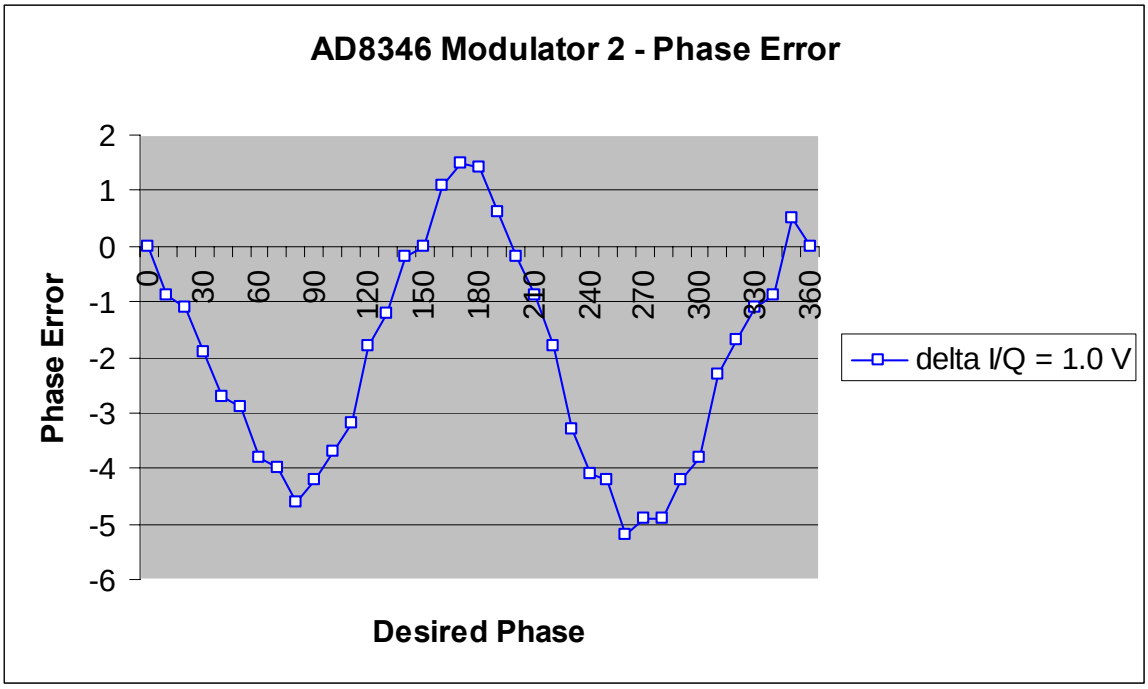

Figure 20. AD8346 Phase error measurements board 2.

2. Demodulator

The Analog Devices AD8347 demodulator evaluation board is used on the receiver side to extract the phase and amplitude from incoming RF signals. This is a broadband direct quadrature demodulator that performs demodulation direct to baseband and covers a frequency range of 0.8 to 2.7 GHz [21]. The incoming RF goes through two gain controlled amplifiers before the mixers, and then separate I and Q channel variable gain amplifiers. The LO is run through two quadrature phase splitters to achieve high accuracy over the entire frequency band. Figure 21 shows AD8347 block diagram and Evaluation Board.

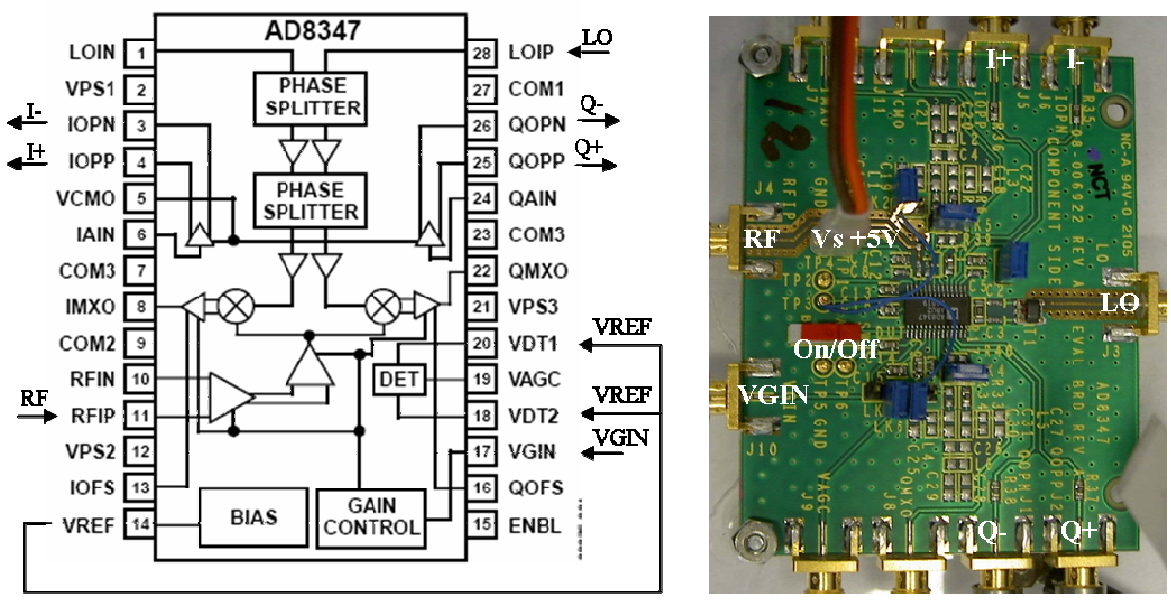

Figure 21. AD8347 block diagram and Evaluation Board (From [22]).

Previous research [10] has shown that the I/Q-channel phase output did not have a linear relation with the RF-input due to the AGC function. The phase values tended to be forced by the AGC towards the axis, instead of giving a circle around the origin. Instead of using the AGC function, the card should therefore be configured for a fixed gain, and this can easily be done by using the VGIN mode. In this mode the gain is controlled with a fixed voltage level attached to VGIN, input J10. Some minor changes to the evaluation board need to be done (Figure 22), where Jumpers LK2, 3 and 6 need to be pulled, and VDT1 and VDT2 wired to TP3.

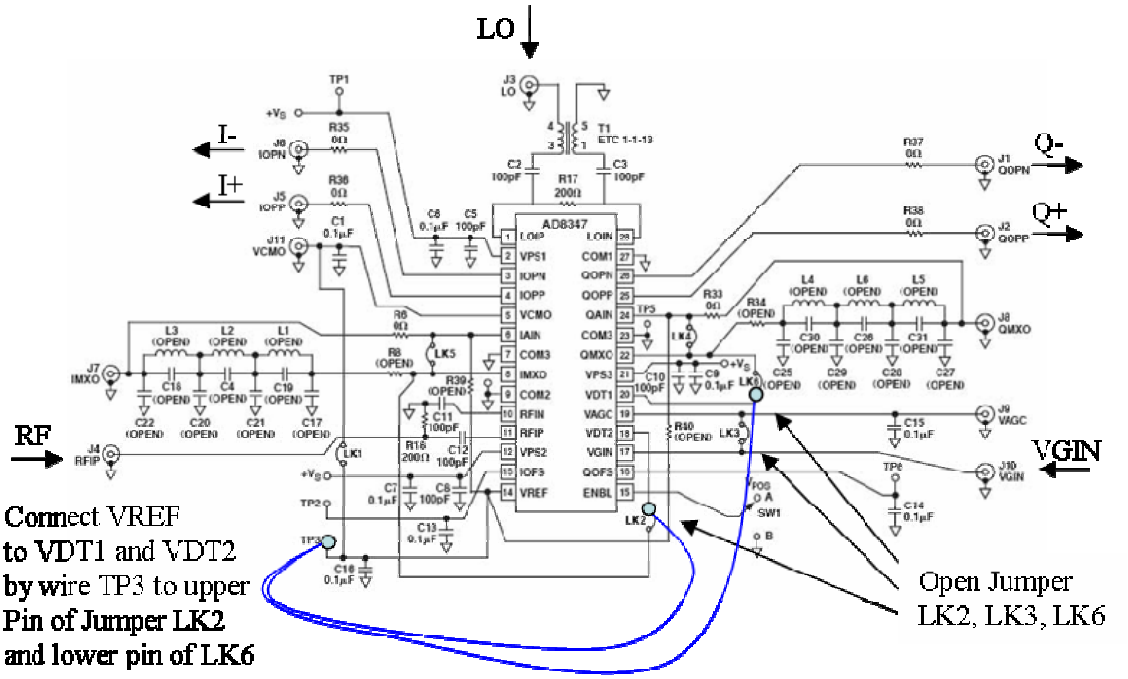

Figure 22. AD8347 Evaluation board schematic (After [22]).

If we look at the VGIN-mode in the block diagram in Figure 23, it is clear that the two input amplifiers are gain controlled by the fixed voltage put on VGIN. Similarly for the separate I and Q channel variable gain amplifiers that follow the baseband outputs of the mixers.

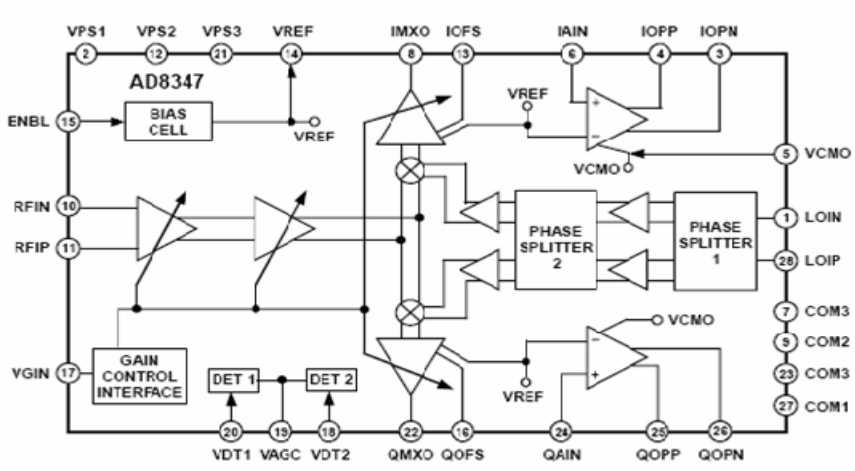

Figure 23. AD8347 block diagram, configured for VGIN (From [22]).

When using the AD8347 in VGIN mode, a fixed voltage level needs to be attached to J10. This input is specified between 0.2-1.2 V and previous research [10] has shown that a VGIN set to 0.38 V will provide the largest I/Q-circle without distorting the differential output.

Measurements of the I/Q-response have shown that each board is unique and has an individual offset of the I/Q-circle from its origin. This offset in I and Q needs to be measured and then used in the Controller as a calibration value for that particular board. This is an important calibration to achieve a 360 degree linear phase response out of the AD8347. Every board needs to be measured before put into operational use, and the setup to measure the AD8347 is shown in Figure 24.

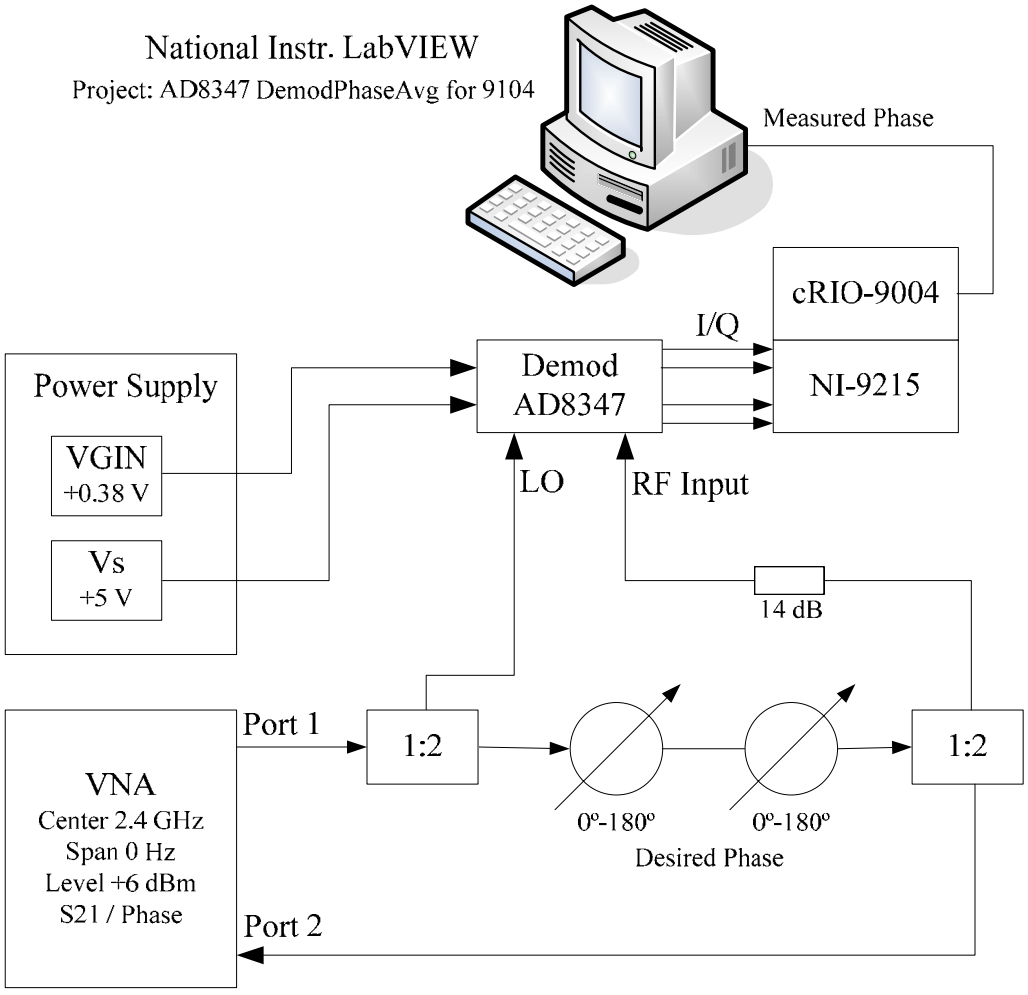

Figure 24. AD8347 Demodulator phase calibration setup.

Preparing the setup for AD8347 demodulator phase measurement takes about two hours, so it is preferable to do all the boards at the same time. The following procedures should be used. First attach the demodulator to the measurement rig; using four screws to fix it in position (see Figure 25). Connect all the coaxial cables and hardware as shown in Figure 24, and use two powers supply to provide the +5 V for Vs, and the +0.38 V for VGIN,

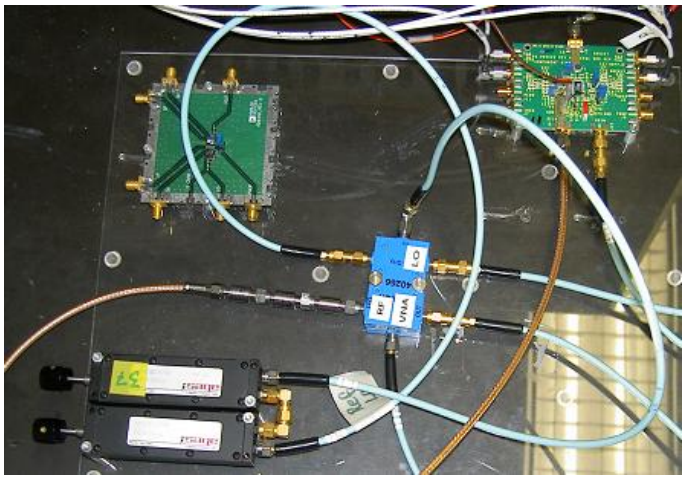

Figure 25. AD8347 Measurement setup.

Next, set the mechanical phase shifters in a default position. This is done by turning the knobs on both shifters counter clockwise until stop. The shifters are mechanically adjustable phase shifters from Sage Laboratories [23], with an insertion loss of 0.7 dB, and a frequency range of dc – 8 GHz (see Figure 26). Each of them can shift the phase 0-180 degrees, and when connected in series, they can be used to sweep the desired phase input of the demodulator from 0 to 360 degrees.

Figure 26. Sage Phase Shifters.

To provide LO and RF, we will use the VNA HP8510C [24]. The front panels are shown in Figure 27. This device should be setup to transmit a 2.4 GHz CW signal, with a power level of +6 dBm on port 1. The other port is then used to measure the phase shift introduced by the two phase shifters. The required VNA settings are listed in Table 1.

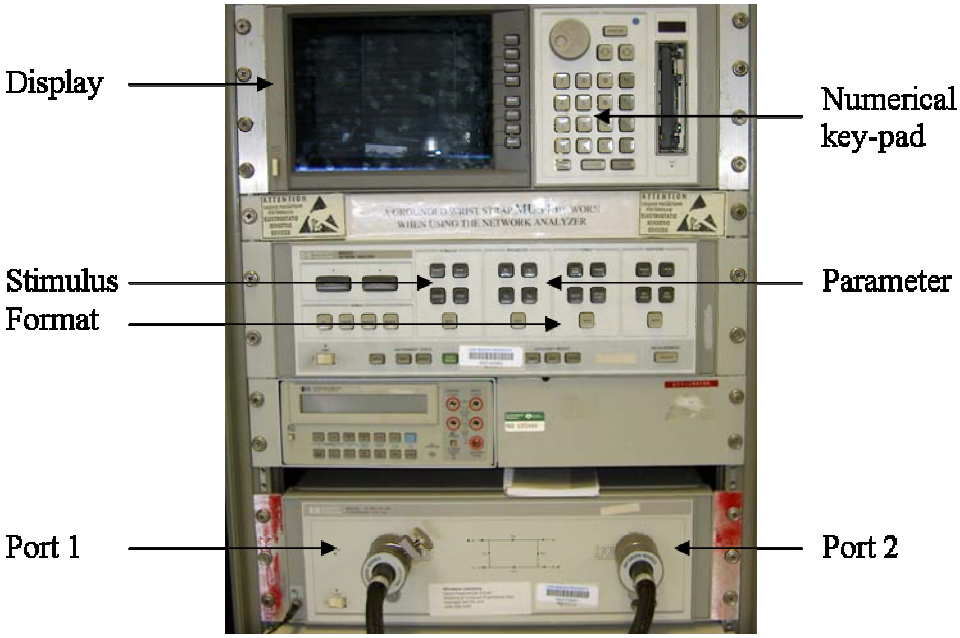

Figure 27. VNA HP 8510C front panel.

Parameter	Setting/Value	Press
Operating frequency	2.4 GHz CW	STIMULUS CENTER 2 . 4 G/n
Span	0 Hz	STIMULUS SPAN 0 x1
Power level	+6 dBm	STIMULUS MENU Port 1 6 x1
Type of measurement	Phase	FORMAT PHASE
S-Parameter	S_{21}	PARAMETER S_{21}
Sweep rate	51	STIMULUS MENU number of points 51
Set start-phase to zero	0	DISPLAY Data to mem 2 Math (./)

Table 1. VNA settings for calibrating the demodulator.

The AD8347 outputs are then used as inputs to the NI-9215 analog to digital module, which is connected to the LabVIEW computer. LabVIEW and project "AD8347 DemodPhaseAvg for 9104.vi" are shown in Figure 28. To choose the right FPGA-module you need to scroll down the "VISA Resource-menu" to find the address "visa://169.254.0.2/RIO0::INSTR". This can take some time due to the handshake procedures that take place between the host and FPGA. To start the program just press the run arrow in the top left toolbar. Data should be taken on the four I and Q average voltage values, every 20 degrees to get enough data to accurately plot the I/Q circle.

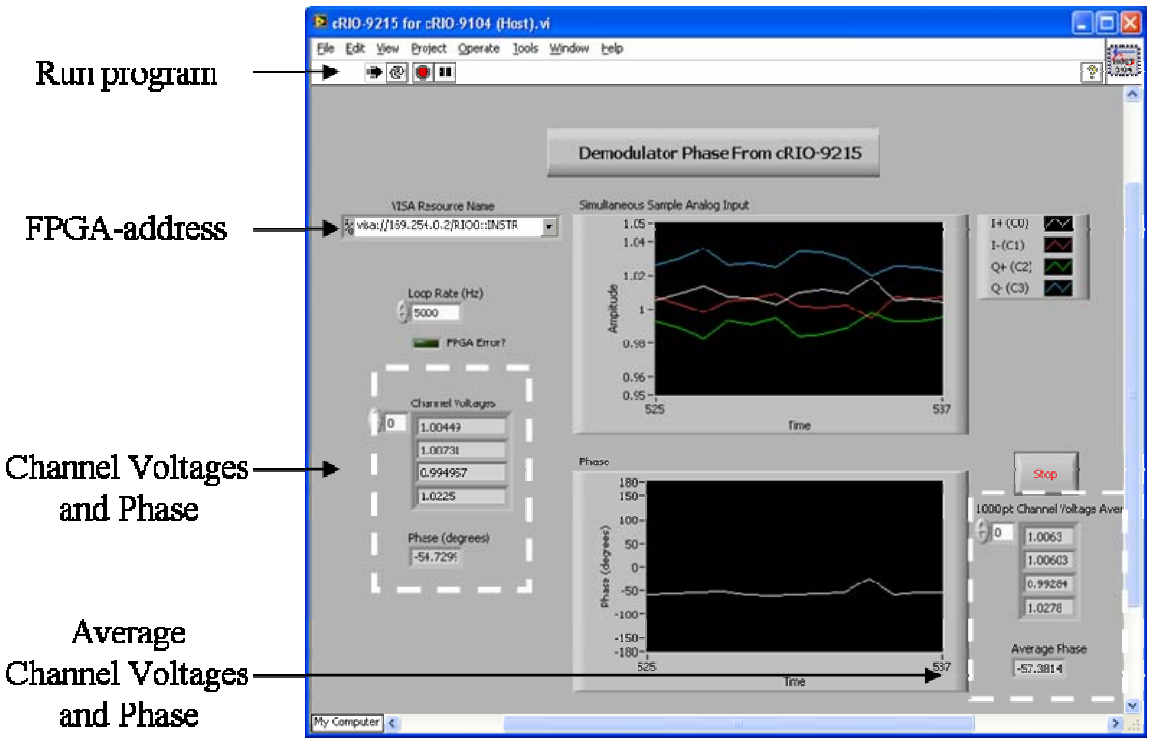

Figure 28. LabVIEW AD8347 Voltages measured by the program "DemodPhaseAvg for 9104.vi".

If the FPGA does not show up on the scroll list, check that the BITE LEDs on the FPGA does not indicate any connection problem with the host, see Figure 29.

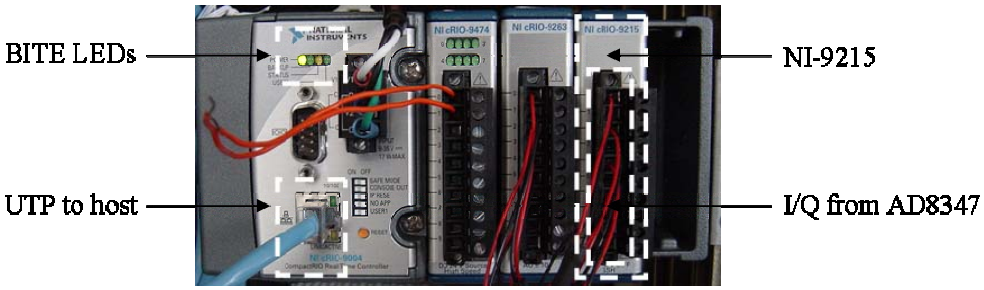

Figure 29. LabVIEW NI-9215.

Measured average channel voltages are then put into an excel spreadsheet and used as input to a MATLAB program from Burgstaller [10], which plots the I/Q-circles and their offsets as seen in Figure 30. It is easy to see on the plots that each board is individual and has its own offset. This means that each board has to be measured, and its offset needs to be part of the MATLAB script used in LabVIEW, at the Controller. The reason for doing this is to get a linear phase response from the AD8347 from 0 to 360 degrees.

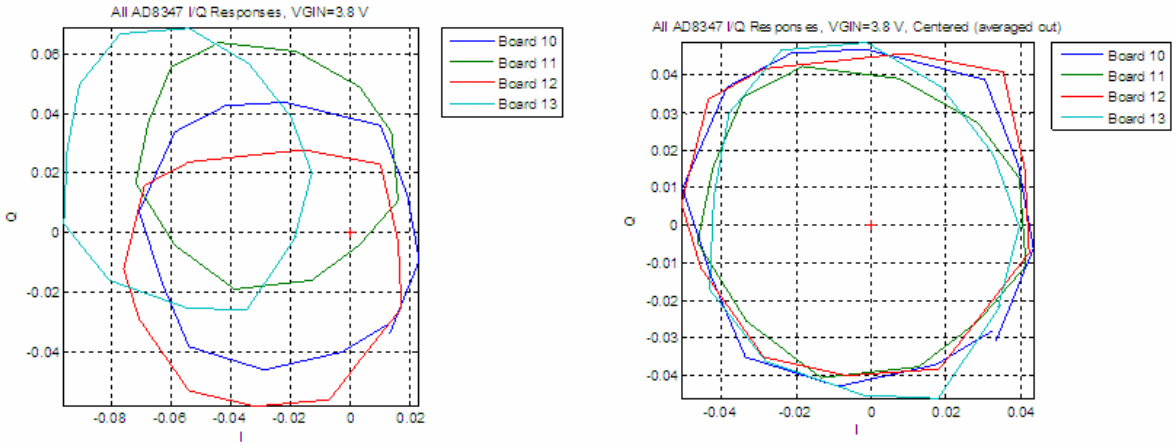

a) Without correction b) With correction

Figure 30. Plotted AD8347 demodulator phase characteristics.

Table 2 shows the I/Q-offset for demodulator boards 10 to 13. These values are then subtracted from the I and Q levels in the MATLAB script, before the average phase calculation is performed.

Board No.	Offset I_0/Q_0 [mV]	Operation
10	I_0 –20.4615 / Q_0 -2.9231	Used in T/R module 1
11	I_0 –25.6923 / Q_0 +21.6923	Used in T/R module 2
12	I_0 –25.3769 / Q_0 -17.7692	Used as reference
13	I_0 –52.9231 / Q_0 +20.2308	Used as spare part

Table 2. AD8347 I/Q-Offset

The MATLAB script used in the Controller software is shown in Figure 31. The offset values for this particular board are -20.2308 mV for I, and -2.9231 mV for Q.

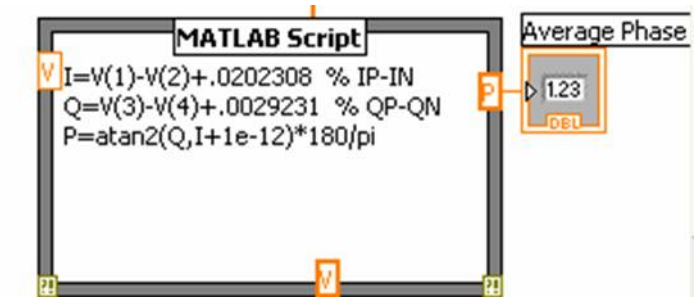

Figure 31. MATLAB Script in Block Diagram for cRIO 9104 (host).

The two T/R modules that are currently in operation for the demonstration setup are boards 10 and 11 and their I/Q-offsets can be seen in Figure 32. The arrows show the magnitude and direction that the offsets need to be applied.

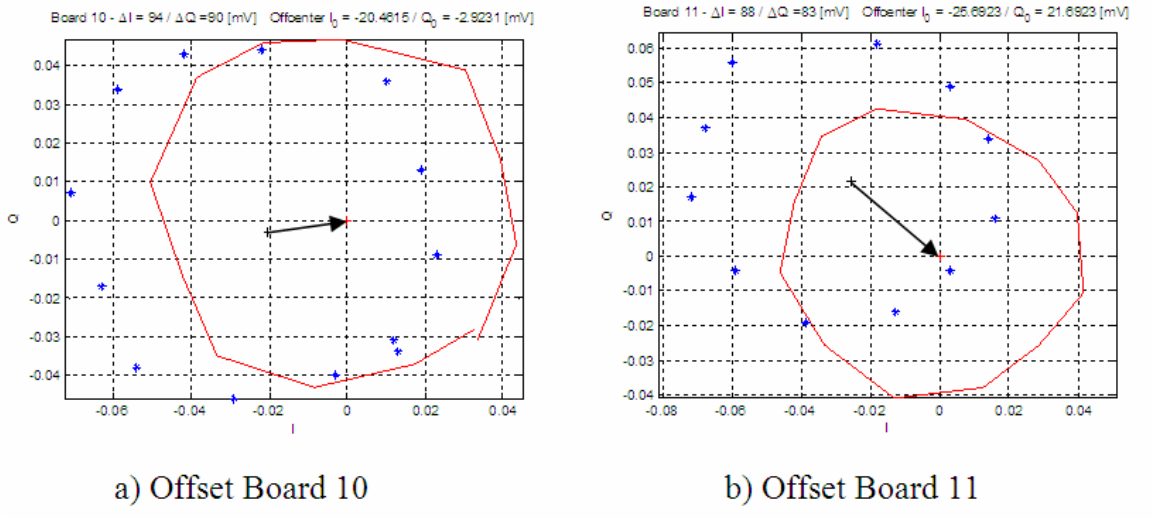

Figure 32. Characteristics of boards 10 and 11.

E. PHASE SYNCHRONIZATION

The concept described as the "brute force" technique is based on a phase shifter implemented in every element. When an element is in the synchronization mode, the LO feedback signal is phase shifted. That shifted LO will then be added together with the un-shifted LO from the reference element back at the Controller. The goal is to shift the phase, so that the difference between the LO from the reference element and synchronized element are 180 degree apart. This will cause a cancellation of the signal, down to a level equal to the difference in amplitude. This level can be monitored, and a search for a minimum, will give the phase difference of 180 degrees. A simple test setup (Setup A in Figure 33) was done with mechanical phase shifters simulating path insertion phase to verify that the detector gives the proper output.

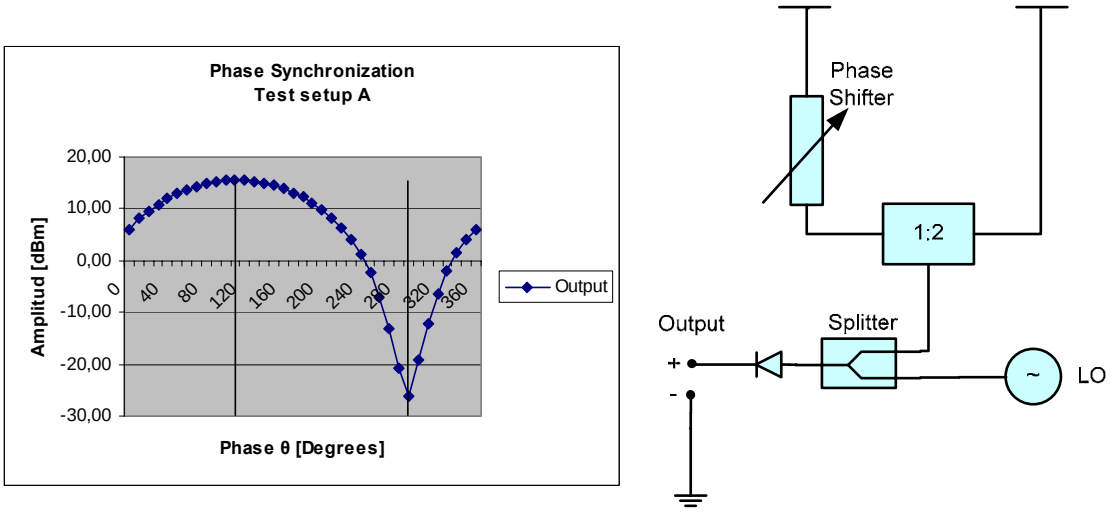

Figure 33. Phase synchronization, setup A.

The detector output was measured with a volt meter and the results are shown in Figure 33. The data showed that a sharp notch makes it easy to find the minimum, i.e., where the phase difference is 180 degrees. The next step was to use the modulator as the phase shifter and LabVIEW to monitor and control the operation. Setup B, discussed in Chapter IV, will include both the AD8346 modulator and a switch to change between synchronization mode and normal mode.

F. SUMMARY

This chapter has analyzed the T/R module, and examined all the current devices involved in a synchronization process. Measurements have been done, and they all show good results using a phase shifter. A revised circuit (setup B), will be examined in the next chapter. Setup B eliminates the phase shifter but requires some new hardware, and measurements were done to have their performance verified before they are put in to the setup.

IV. HARDWARE AND SOFTWARE DEVELOPMENT

This chapter describes the developments in several key areas of synchronization and data communication. They include breadboarding and validation of the synchronization circuit, development and testing of the LabVIEW Controller software, and integration of these into the existing T/R modules built by Yeo [11].

The revised architecture for the T/R module is shown in Figure 34. The switch is positioned to the "LO 2.4 GHz" branch when in the synchronization mode. Otherwise it is switched to the power amplifier (PA). Wireless data communication and control uses the 5.8 GHz antenna.

The LO signal is received from the Controller and is input to the modulator. The modulator introduces phase shift based on the received LO phase and sends it back to the Controller for comparison with the reference. The reference and returned (phase shifted) LO are compared in a detector to find the phase shift that results in a minimum. This phase value plus 180 degrees is the phase needed to synchronize the T/R module to the master.

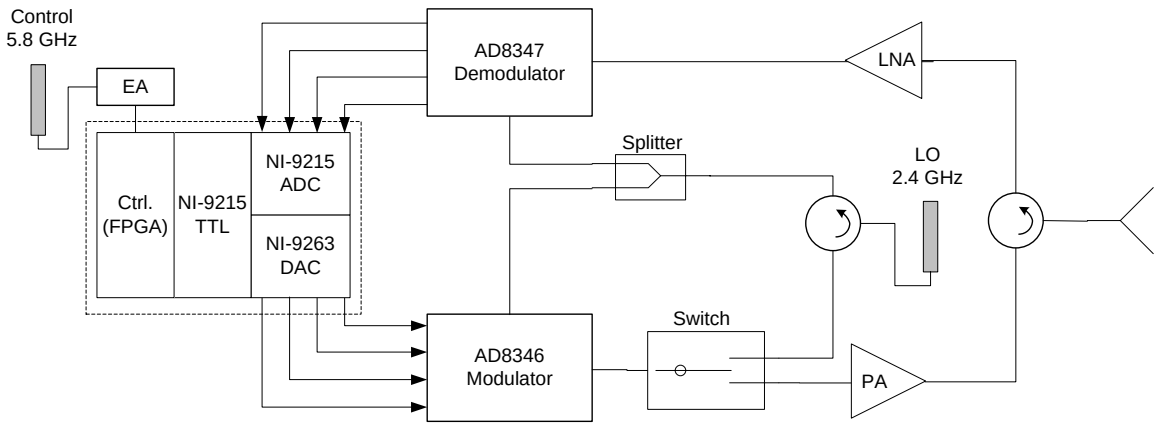

Figure 34. T/R module with integrated synchronization circuits.

A. BACKGROUND

To validate the sync circuit a breadboard test was performed using setup B, shown later in Figure 43. Setup B requires a circulator, switch and switch-control hardware. These new devices were first measured and verified against their manufacture's specifications before being incorporated into the setup. But setup B is completely wired, and just one step towards a wireless phase synchronization concept. Later the wired connections will be replaced by a SOHO wireless network.

B. T/R MODULE

The upgraded T/R module design with integrated synchronization function needs an extra circulator and a switch. These two devices are shown with dashed lines in the block diagram in Figure 35. The switch is used to select between the sync mode and normal mode, and the circulator simultaneously provides LO input and phased shifted LO output, at the LO 2.4 GHz antenna.

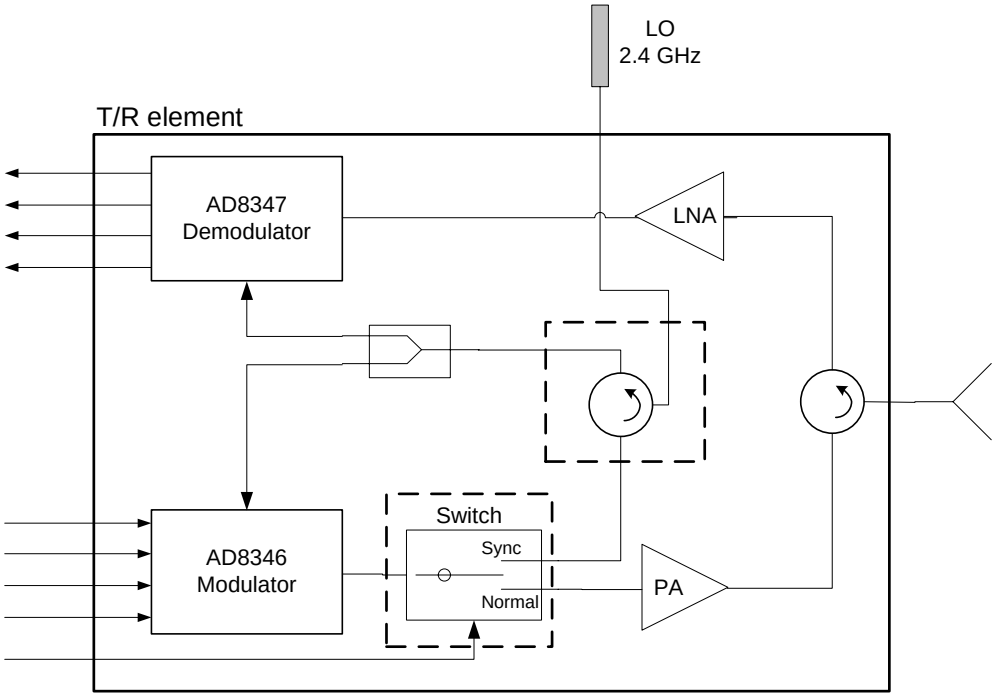

Figure 35. Upgraded T/R module block diagram with sync hardware.

1. Circulator

An extra circulator for the synchronization function is needed in each T/R module. The same circulator model as the one currently being used to separate transmit from receive is also used for this purpose as shown in Figure 36. The model is D3C2040 from DiTom Microwave [25] as shown in Figure 37.

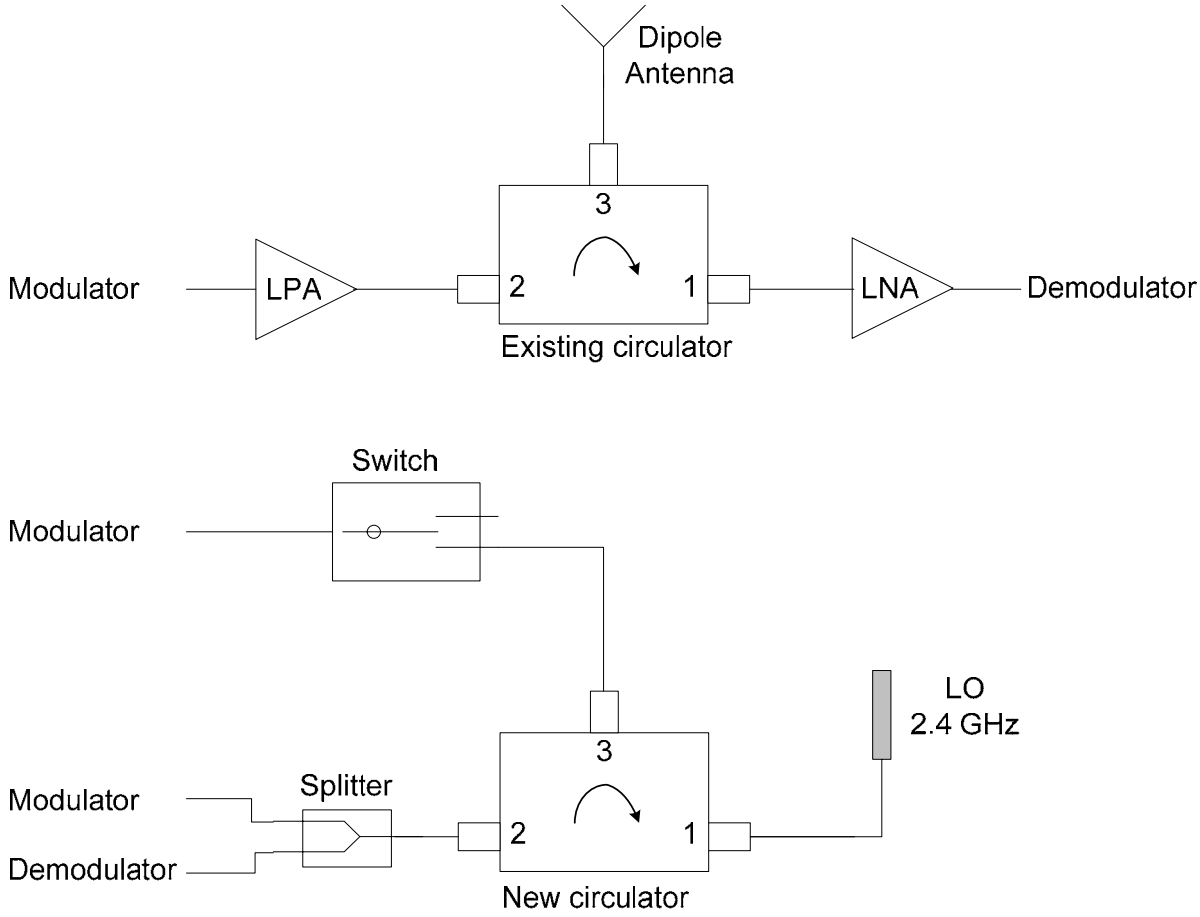

Figure 36. Principal mechanical layouts for the existing and new circulator.

Figure 37. Circulator from DiTom Microwave.

Isolation and insertion loss where measured for the two new circulators, and they matched the manufacture's specification [25]. Measured data can be seen in Table 3, and return loss and insertion loss plots are shown in Figure 38.

Parameter	Specified	Measured at 2.4 GHz				Unit
		Circ#	Port 1→2	Port 2→3	Port 3→1	
Isolation, S12	20 Typically	1447	22.087	20.438	21.034	dB
	18 Minimum	1448	21.160	20.037	19.975	
Insertion Loss, S21	0.40 Typically	1447	0.3986	0.4192	0.4148	dB
	0.50 Maximum	1448	0.3823	0.4355	0.4211	

Table 3. Specified and measured parameters for new circulators.

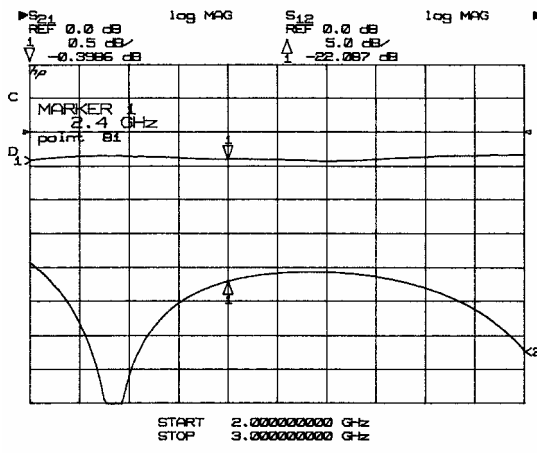

(a) Circulator S/N 1447, Port 1 → 2

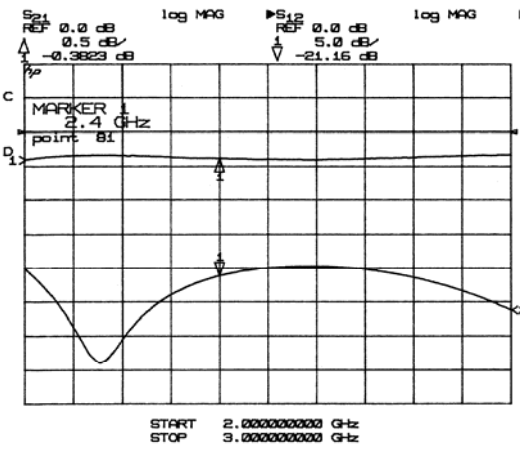

(b) Circulator S/N 1448, Port 1 → 2

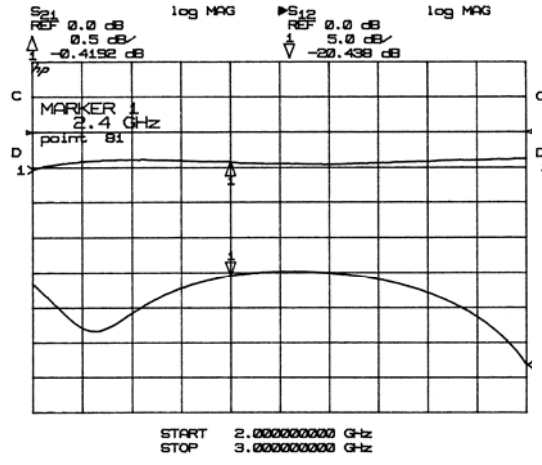

(c) Circulator S/N 1447, Port 2 → 3

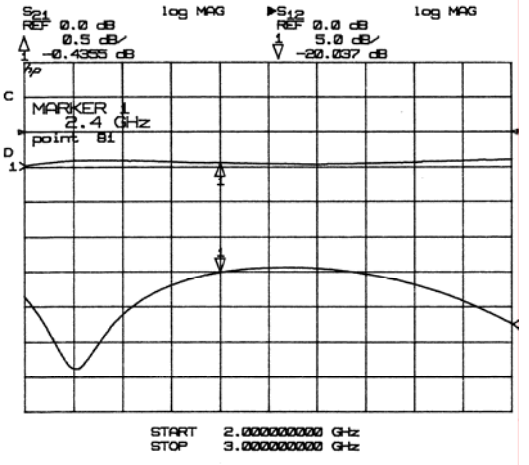

(d) Circulator S/N 1448, Port 2 → 3

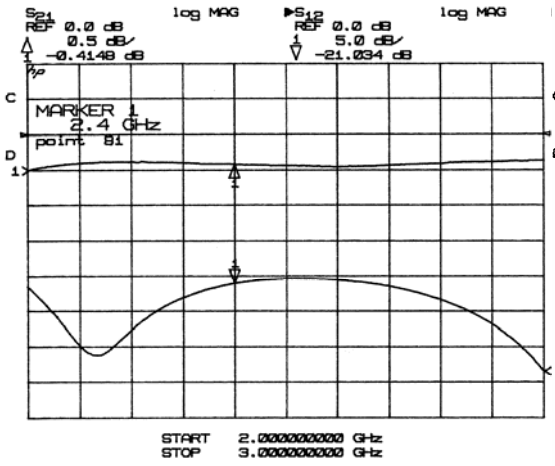

(e) Circulator S/N 1447, Port 3 → 1

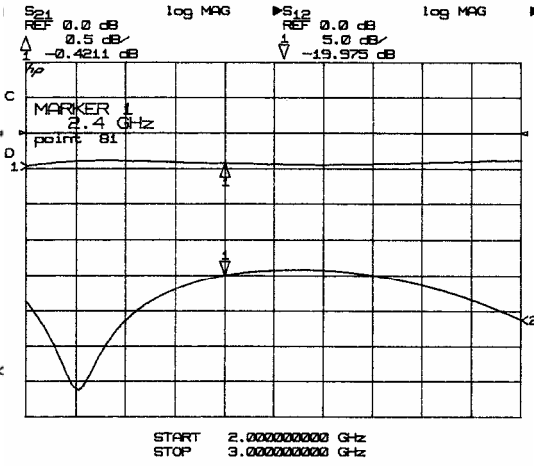

(f) Circulator S/N 1448, Port 3 → 1

Figure 38. Circulator measurements of S21 and S12.

2. Switch

A switch is needed to change between the sync and normal operating modes for the T/R elements. The switch chosen is a high isolation, 50 ohms, DC to 5 GHz, Single-Pull Double-Throw (SPDT), with TTL driver from Minicircuits [26] shown in Figure 39.

Figure 39. ZASWA-2-50DR Switch.

The switch is of absorptive type and terminates the unused port through a grounded 50 ohm resistor, which gives a good standing wave ratio (SWR). It also has a built-in TTL-driver, which makes it possible to control the switch with simple voltage switching (see Figure 40). Isolation, insertion loss and SWR were measured for the two new switches and the data plots can be seen in Figures 41 and 42.

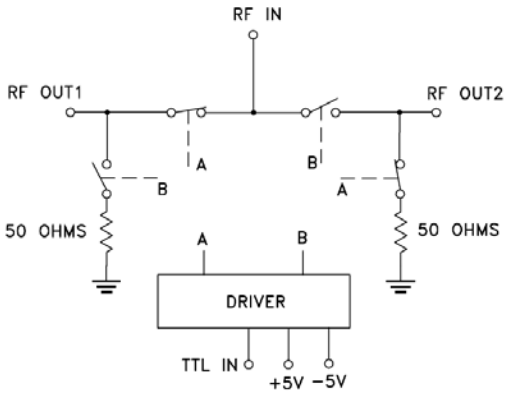

Figure 40. Switch ZASWA-2-50-DR, Electrical schematic (From [26]).

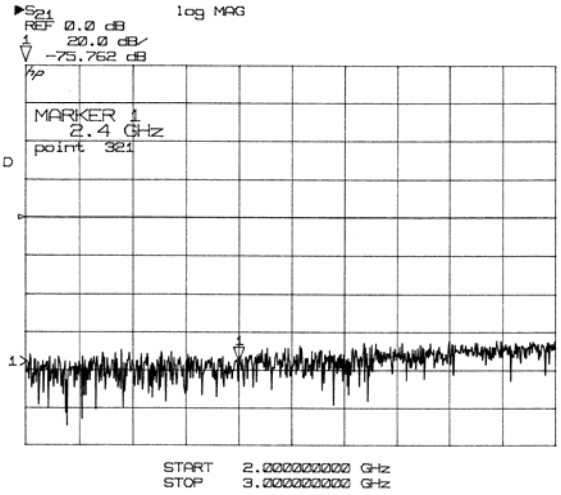

(a) log MAG $RF_{in} \rightarrow RF_{out}1$, TTL high

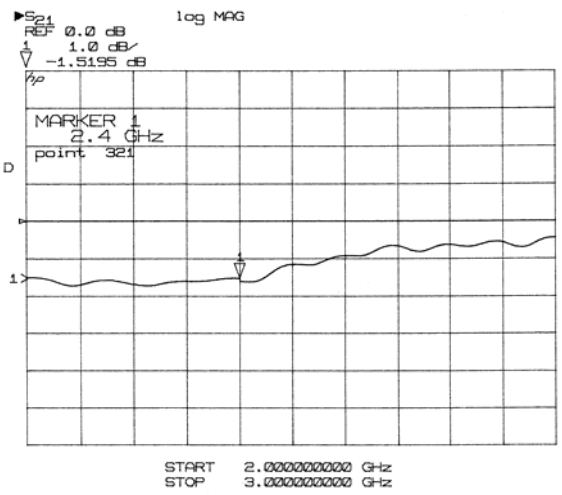

(b) log MAG $RF_{in} \rightarrow RF_{out}1$, TTL low

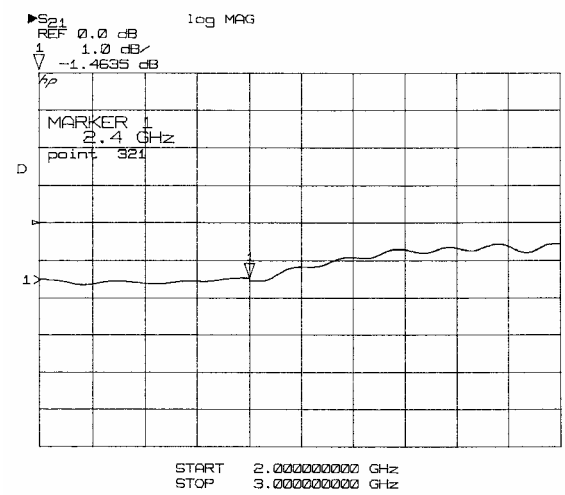

(c) log MAG $RF_{in} \rightarrow RF_{out}2$, TTL high

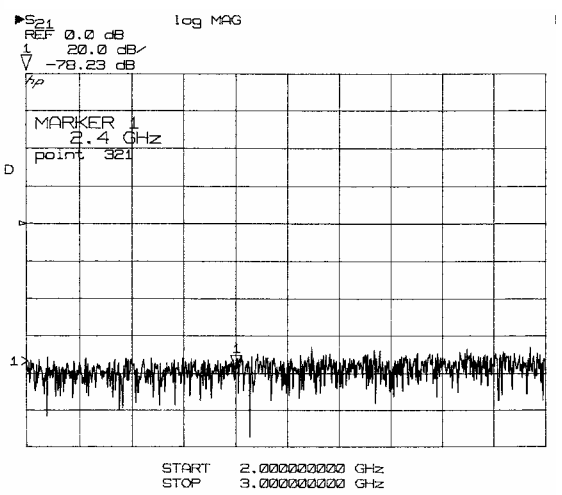

(d) log MAG $RF_{in} \rightarrow RF_{out}2$, TTL low

Figure 41. Switch measurements of S21.

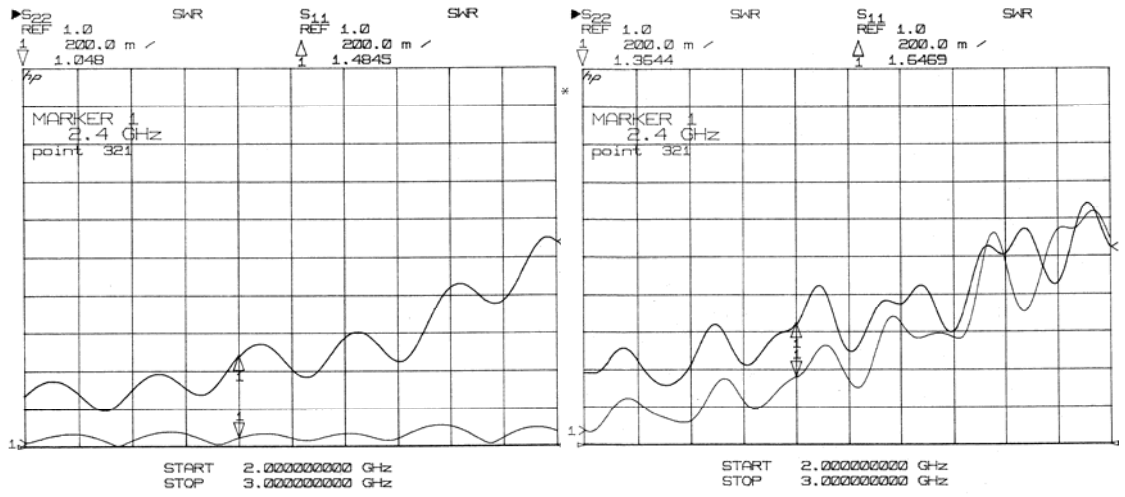

(a) SWR $RF_{in} \rightarrow RF_{out}1$, TTL high (b) SWR $RF_{in} \rightarrow RF_{out}1$, TTL low

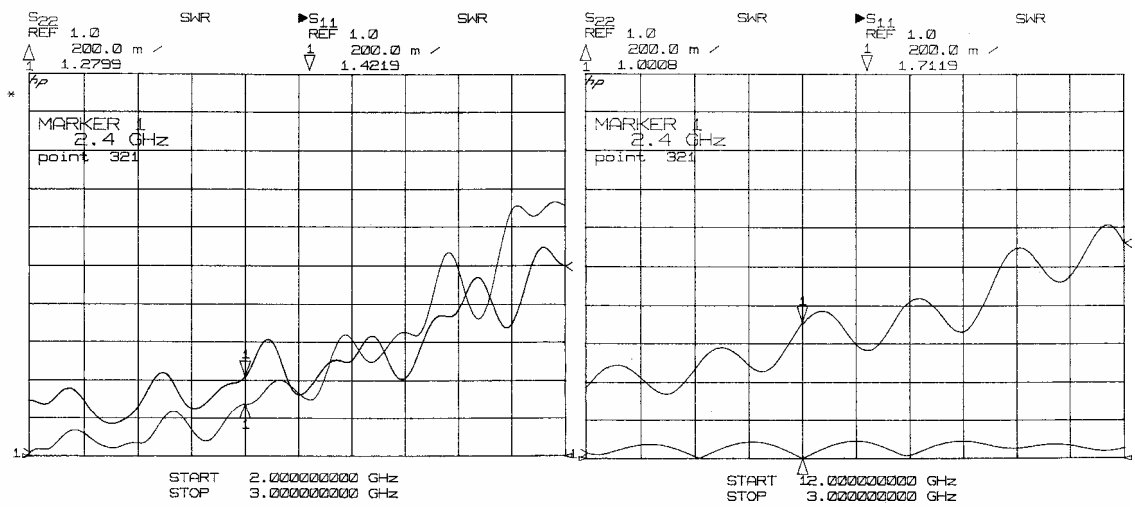

(c) SWR $RF_{in} \rightarrow RF_{out}2$, TTL high (d) SWR $RF_{in} \rightarrow RF_{out}2$, TTL low

Figure 42. Switch measurements of S22 and S11.

C. PHASE SYNCHRONIZATION

1. Reduced Concept

The purpose of setup B is to verify that the new devices could perform in a synchronization circuit before they where implemented in the T/R modules. In this setup the NI-9263 analog output is used for control of the AD8346 modulator. The signal from the modulator is then run through the switch and the circulator before it is added together with the same LO signal in the detector. In Figure 43 the path A + B represents propagation from the Controller to the module being calibrated and back. The path C represents propagation from the Controller to the reference module and back. The summed voltage level is then measured for every 10 degrees phase shift of the modulator and the resulting plot is shown in Figure 44.

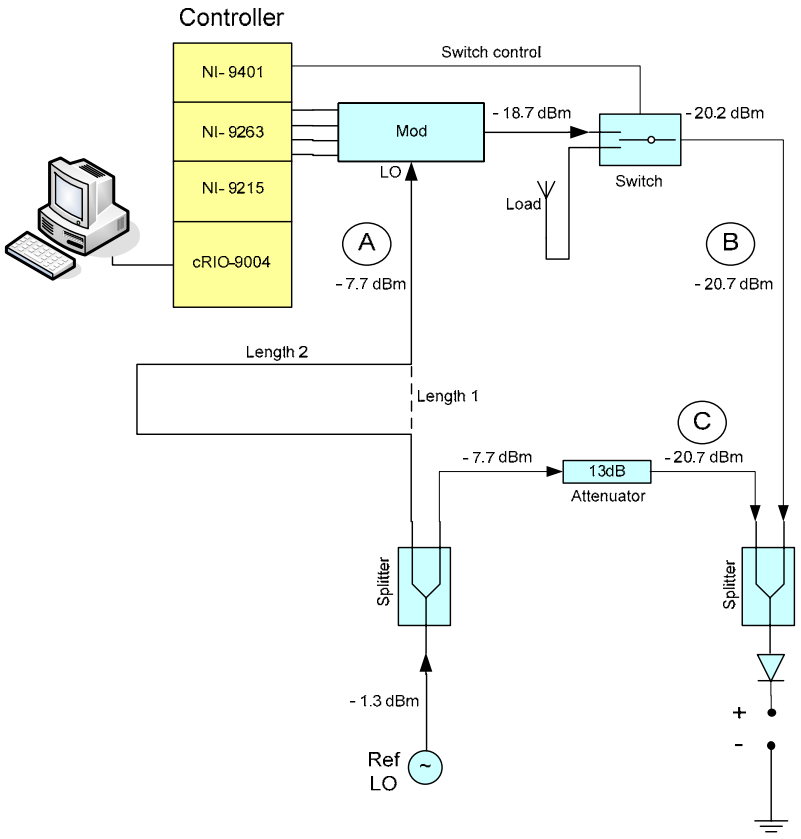

Figure 43. Phase synchronization, setup B.

The measurements where done with two different cable lengths, where length 2 was 20 mm longer than length 1. Since the wavelength for 2.4 GHz is 0.125 m, a 20 mm change in length should change the peak minimum 57.6 degrees. The theoretical calculation is verified by the measurements shown in Figure 44. The deep null assures that an accurate measurement of the phase difference can be made. Later the hardwire paths will be replaced by free space links.

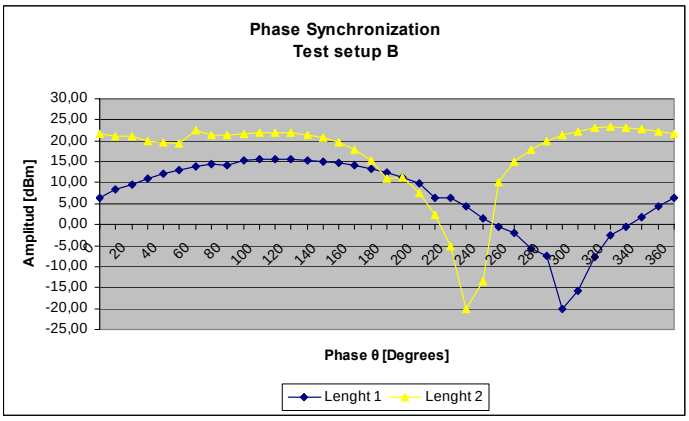

Figure 44. Phase synchronization result for setup B.

The result verifies that the new devices function as expected and the synchronization circuit can be integrated into the upgraded T/R modules. The extra circulator and switch were put into the old T/R modules, and new cables where made for interconnection as shown in Figure 45.

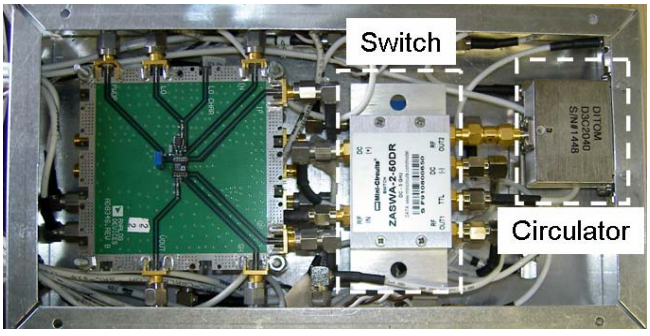

Figure 45. Upgraded T/R module with synchronization circuit.

2. Full Array with Wired LO Distribution

Before attempting the full demonstration of wireless phase synchronization, a wired setup was used to verify the new hardware installation. Instead of the free space channel for LO distribution, cables where used to connect the 2.4 GHz reference signal to the T/R modules as shown in Figure 46. This test configuration is referred to as setup C.

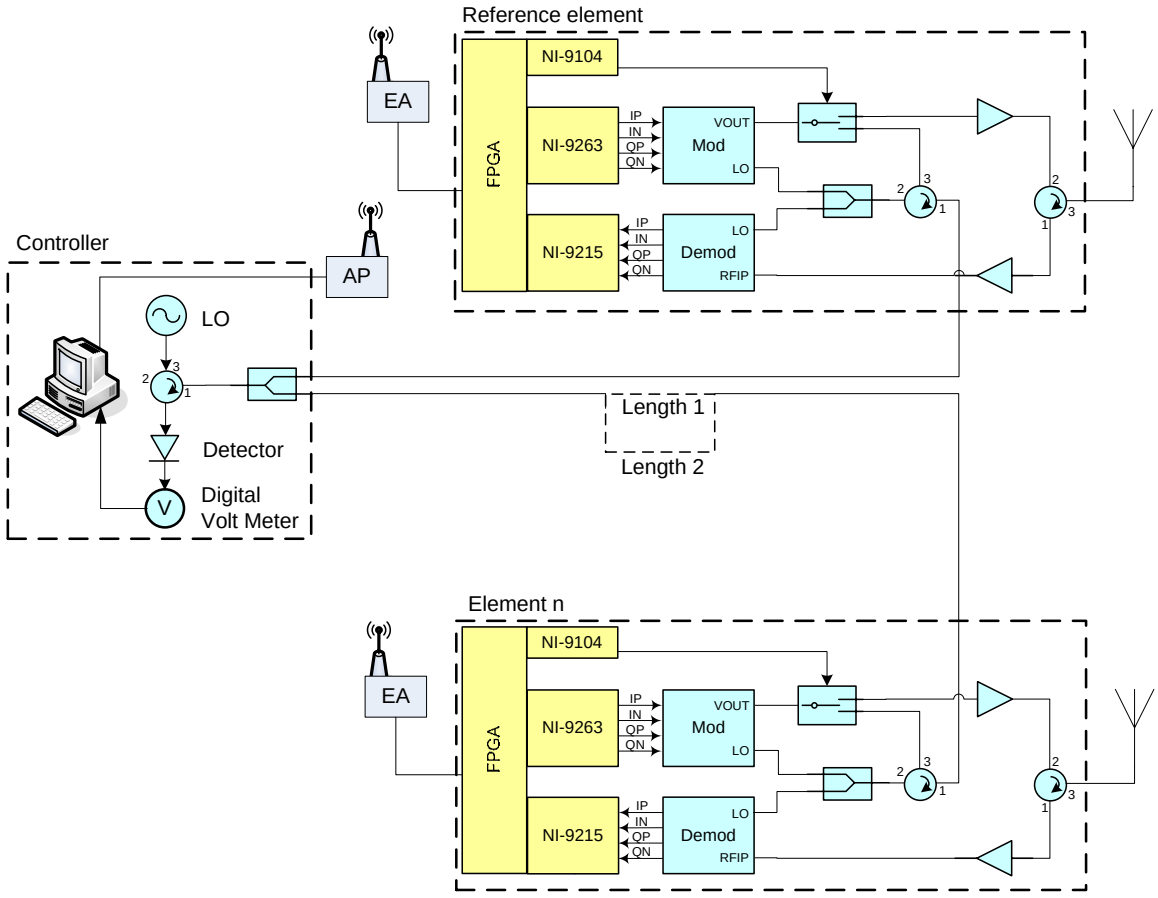

Figure 46. Phase synchronization, setup C.

The measurements where done, as in setup B, with two different cable lengths, where length 2 was 14 mm longer than length 1. Since the wavelength for 2.4 GHz is 0.125 m, 14 mm change in length should change the peak minimum 40.3 degrees. The theoretical calculation was verified by the measurements shown in Figure 47. Ideally the amplitude curves in Figure 47 should be cosine types of functions. The distortion from the ideal is likely due to amplitude intolerance or mismatch at the Controller Antenna. LO signal reflected at the antenna input circulates directly to the detector.

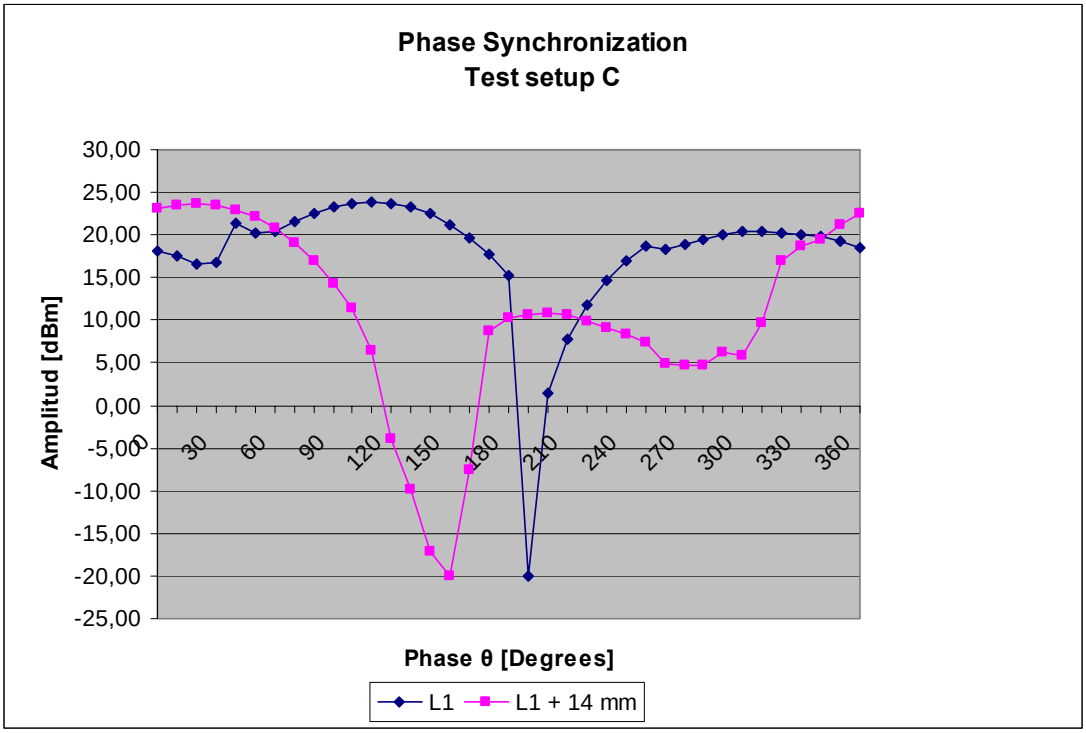

Figure 47. Phase synchronization result, setup C.

D. WIRELESS NETWORK

1. Network Function

The beamforming concept has already been discussed briefly in Chapter III. Basically a SOHO wireless local area network (WLAN) provides a connection between the Controller and the two elements in the demonstration array as shown in Figure 48. The wireless network challenges are being addressed further in a related thesis [13].

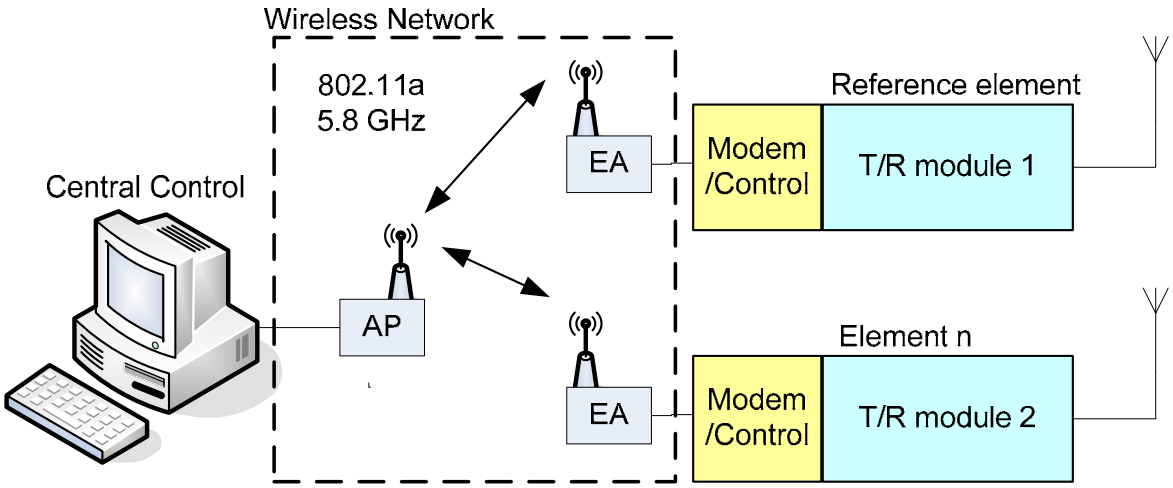

Figure 48. Wireless Network for Communication between the Controller and Modulator.

For the demonstration array the data rate requirements are moderate, however delay through the network (latency) is a concern. Data must be delivered to the Controller in close to real time so that beam processing can be done.

2. Access Point

The access point used is a Tri-Mode Dualband 802.11a/b/g Wireless Access Point from D-Link, with product name DWL-7200AP [27] as shown in Figure 49. It supports both 2.4 GHz and 5.8 GHz. The higher frequency was selected to avoid potential interference with the LO at 2.4 GHz. It has a maximum output power of 18 dBm and a receiver sensitivity of -71 dBm. The manufacturer specifies an outdoor signal range of 328 ft at 54 Mbps, but this signal range and throughput is given under perfect conditions. If used in a rough signal environment, or when you do not have line of sight between units the rate is lower. It also provides Power over Ethernet (PoE), which gives the possibility to install the device at a better location than where the power outlets are.

The configuration interface is easy to manage through the Ethernet connection. In a web browser connect to IP-address 192.168.0.50 and follow on screen instructions. If your computer does not have its IP address within the same range, 192.168.0.XX, you will need to change that by going into the control panel, and assigning a static address to your network interface card (NIC). Do that under Network Connection/Local Area Network/Internet Protocol and TCP/IP. Under properties, uncheck "*Obtain an IP Address automatically*" and then pick your own. Remember also to shut off the 802.11b/g transmitter, and just use 802.11a. Otherwise the LO signal may suffer interference.

Figure 49. D-Link Access point (From [27]).

3. Ethernet Adapter

The Ethernet adapter or Wireless Bridge is from 3COM [28] and is shown in Figure 50. It is also a Dualband device, but as with the access point, we only use the 802.11a standard. The maximum output is 16 dBm, and receive sensitivity at 54 Mbps is -68 dBm. Even if the access point does not use 2.4 GHz, the Ethernet Bridge will keep its receiver on to scan for beacons in both frequency bands, and since the lower band is commonly used in office areas, it will likely find an access point at 2.4 GHz and associate to it. This will cause interference with the LO, and it is necessary to configure the bridge to be fixed at 5.8 GHz.

To set the bridge for fixed mode, go through the same procedures with this bridge as with the access point. Connect the computer to the Ethernet port and go to 169.254.2.2 with a web browser, login as admin with a blank password. Uncheck "*Auto select*" under "*Radio Mode*", and choose 802.11a. This will force the bridge to stay at 5.8 GHz.

Figure 50. 3COM Ethernet Bridge.

E. CONTROLLER SOFTWARE

1. LabVIEW

To control the demonstration setup a user interface was developed in LabVIEW. This interface had to be made from the ground up, because of new hardware and control flow. The new interface is able to control each T/R module's transmitter and receiver separately. The LabVIEW front panel is shown in Figure 51. The detailed functional description of the software appears in [13].

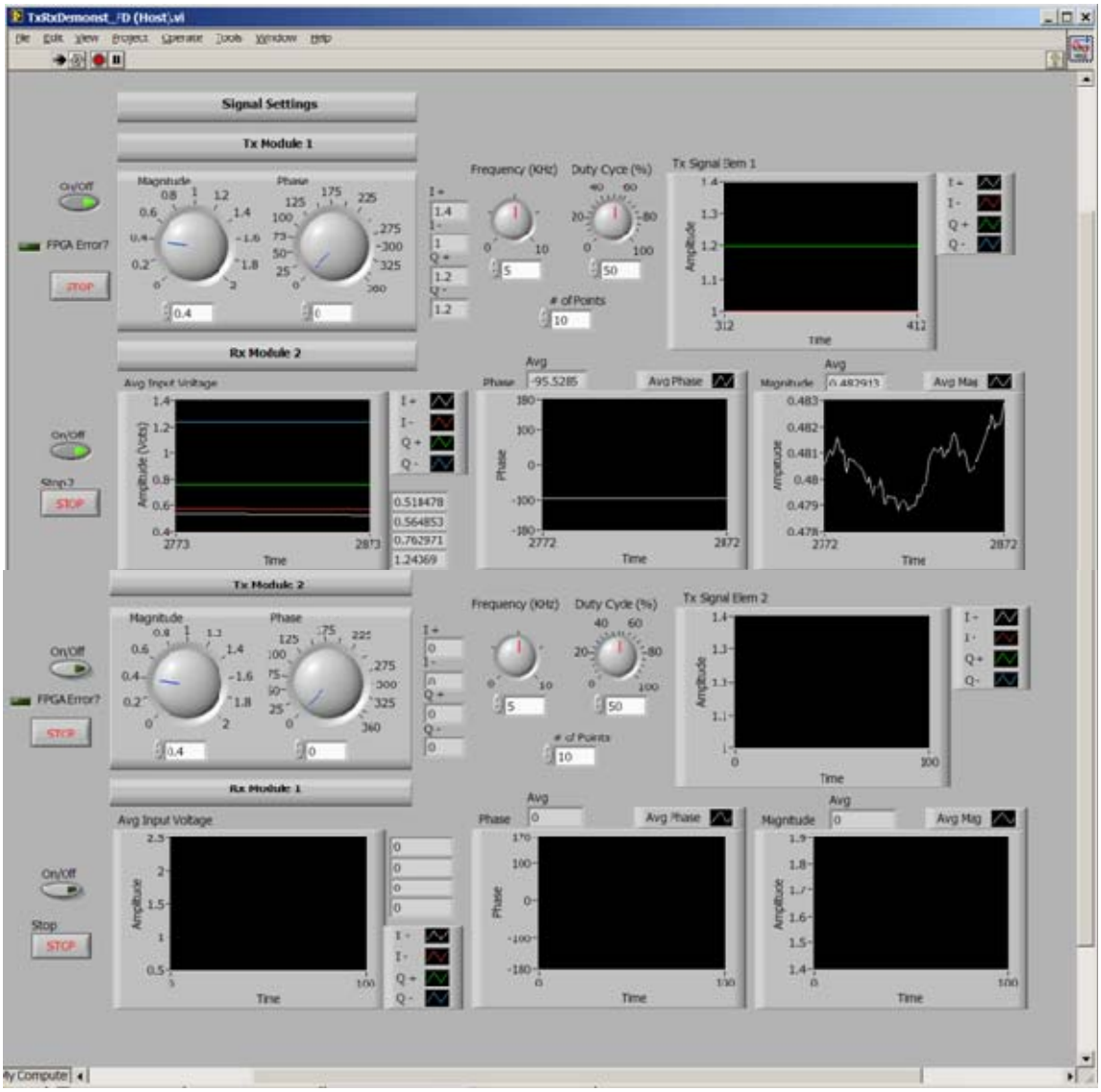

Figure 51. LabVIEW interface for demonstration setup.

2. Switch Control

Control of the synchronization switch within each T/R module, requires a digital output device in the FPGA chassis. The NI-9401 is an 8-channel ultrahigh-speed digital I/O with 5 V/TTL outputs as shown in Figure 52. This output device can be controlled from the LabVIEW program at the Controller.

Figure 52. NI-9401 TTL digital output (From [29]).

3. Detector

The detector adds the two LO signals, one from the reference module and the other from the module being synchronized, and then feeds the dc level to a volt meter. This dc level is then used for detection of the 180 degree phase difference between the two elements. In the demonstration setup a detector from Wiltron [30] is used as shown in Figure 53.

Figure 53. RF Detector Model 75S50 from Wiltron.

F. SUMMARY

This chapter has analyzed the device parameters such as transmission loss, isolation and reflection for the new hardware that will form the synchronization unit. A revised circuit (setup B), has been examined. The purpose of setup B was to verify that the new devices could perform in a synchronization circuit before they where implemented in the T/R modules. The result from the measurements verified that the new devices function as expected, and the synchronization circuit was integrated into the new T/R modules. Before attempting the full demonstration of wireless phase synchronization, a wired circuit (setup C) was used to verify the new hardware installation. The measurements where done, as in setup B, and the theoretical calculation was verified by the measurements.

The next chapter will use the free space channel instead of cable for the LO and phase synchronization, and a wireless test configuration (setup D) will be examined.

V. DEMONSTRATION

A. BACKGROUND

Measurements and results from setup C verified that the phase synchronization concept is operational. The goal is to use the free space channel instead of cable for the LO and phase synchronization. A wireless test configuration (setup D) is needed to verify against that goal.

B. MEASUREMENT

Setup D was configured as in Figure 54 and all the power levels where adjusted to be in the proper ranges. The LO Signal Generator (source) output power level was set to +15 dBm to meet the specified input requirement for the LO at the boards, which is -8 dBm. This level was measured when the LO antennas were within one meter apart. When a greater distance is needed, antennas with higher gain are preferable. The output level from the modulator is only -7 dBm and after it has passed through the switch and circulator the power level is only -10 dBm. The phase shifted LO power level leaving the T/R module is therefore low compared to the source LO that is received. This means that the returned LO (from the modules) is setting the range limit between the source LO antenna and the T/R module LO antenna. An output power level of -10 dBm gives a very short range (<1 m) between the antennas and it needs to be extended in the future.

Even though the antennas had to be close to each other, the measurements from setup D showed that the concept was operational (see Figure 55). We are able to provide wireless LO to the T/R modules, and to perform phase synchronization over the free space channel. The next step is to achieve a higher power level for the T/R modules phase shifted LO signal so that they can be separated further from the source.

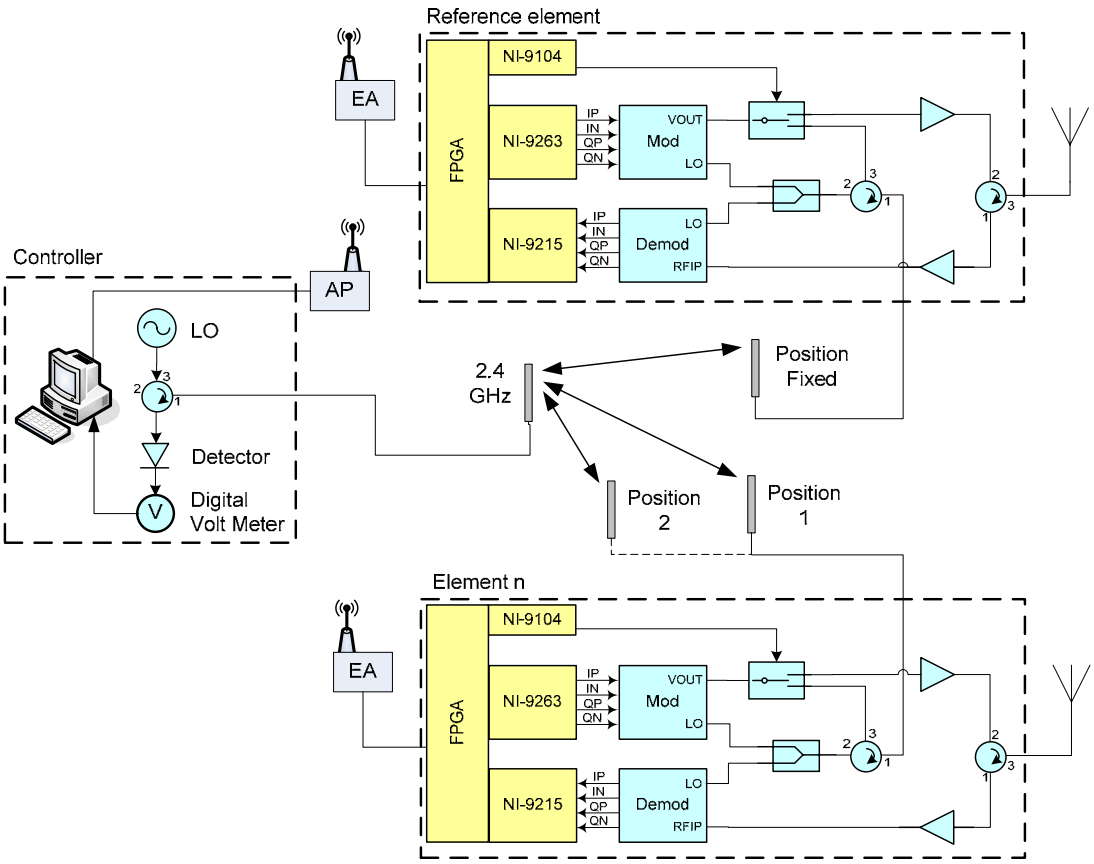

Figure 54. Phase synchronization, setup D.

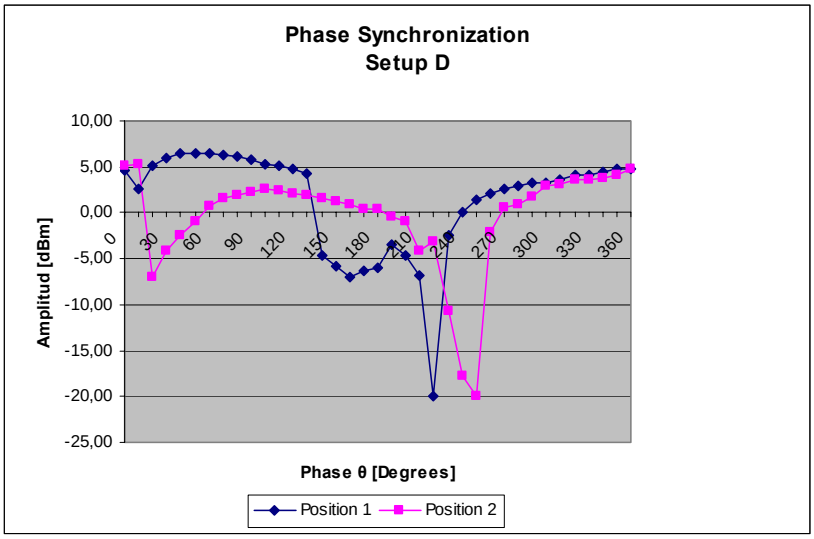

Figure 55. Phase synchronization result, setup D.

To achieve a higher output power level from the T/R modules we need to amplify the RF output signal. A solution to that could be to interchange the PA and switch in the current module. That will place the PA as an amplifier for the LO feedback signal in the sync mode, as well as an amplifier for the transmitted signal in normal mode, as shown in Figure 56. The configuration is referred to as setup E and can be seen in Figure 57.

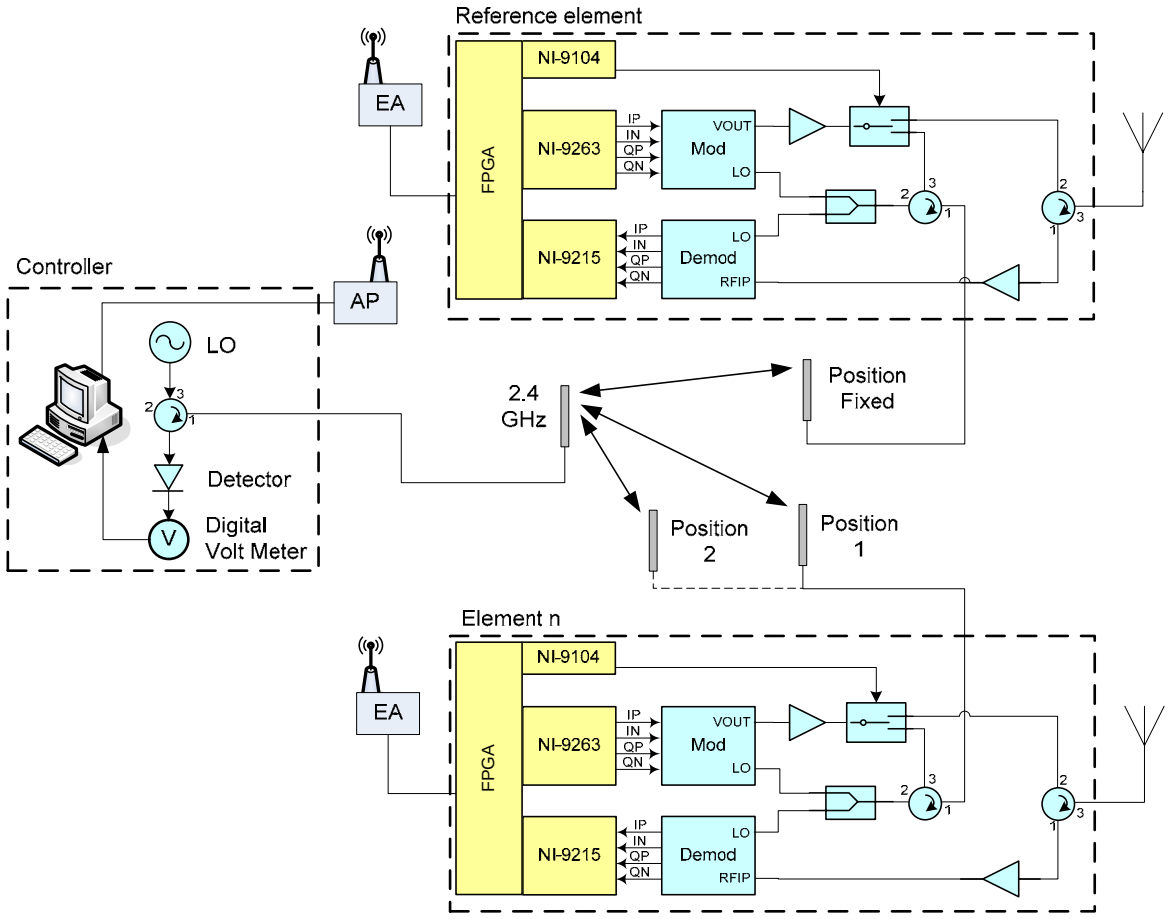

Figure 56. Phase synchronization, setup E.

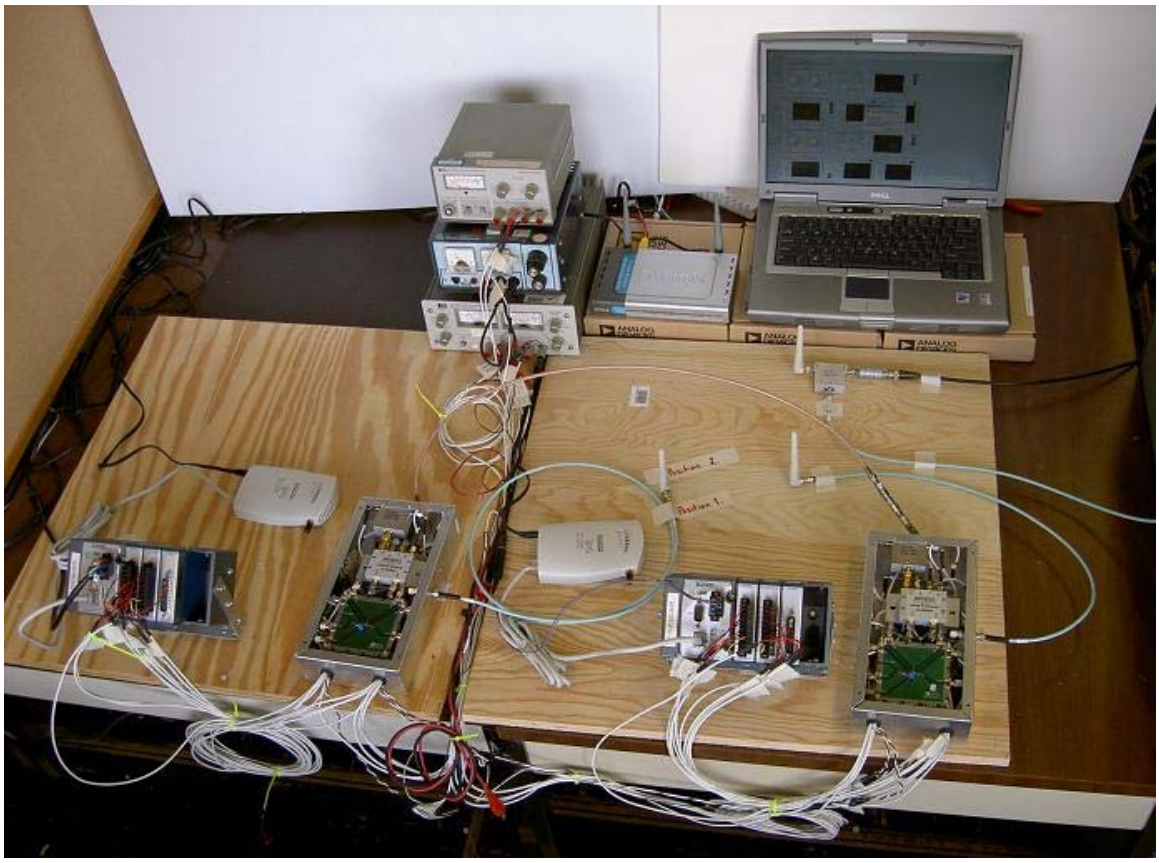

Figure 57. Phase synchronization, setup E.

The result of the measurements from setup E did not turn out as well as those from setup D. When moving the amplifiers into the sync circuit errors were introduced. The notch between the minimum and maximum level out of the detector was not as large, however, it is still possible to find a minimum and change its position by moving the LO antenna of the element being synchronized. This showed that the concept was successful but that there was a problem with the signal levels.

An examination of what caused the problem was conducted. All the power levels were measured and it was concluded that the modulator feedthrough leakage through the circulator was the probable cause. If we look in Figure 58 and follow the signal from the modulator through the circulator it is clear that 21 dB isolation from port 3 to 2 is not enough. Phase shifted LO is fed back into the modulator LO input together with source LO. This would not have been a problem if the two signals were more separated in power

level. The phase shifted LO is only 7 dB lower than the source LO which affects the modulator reference phase. One solution to this problem could be to increase the circulator isolation which is a recommendation for future work.

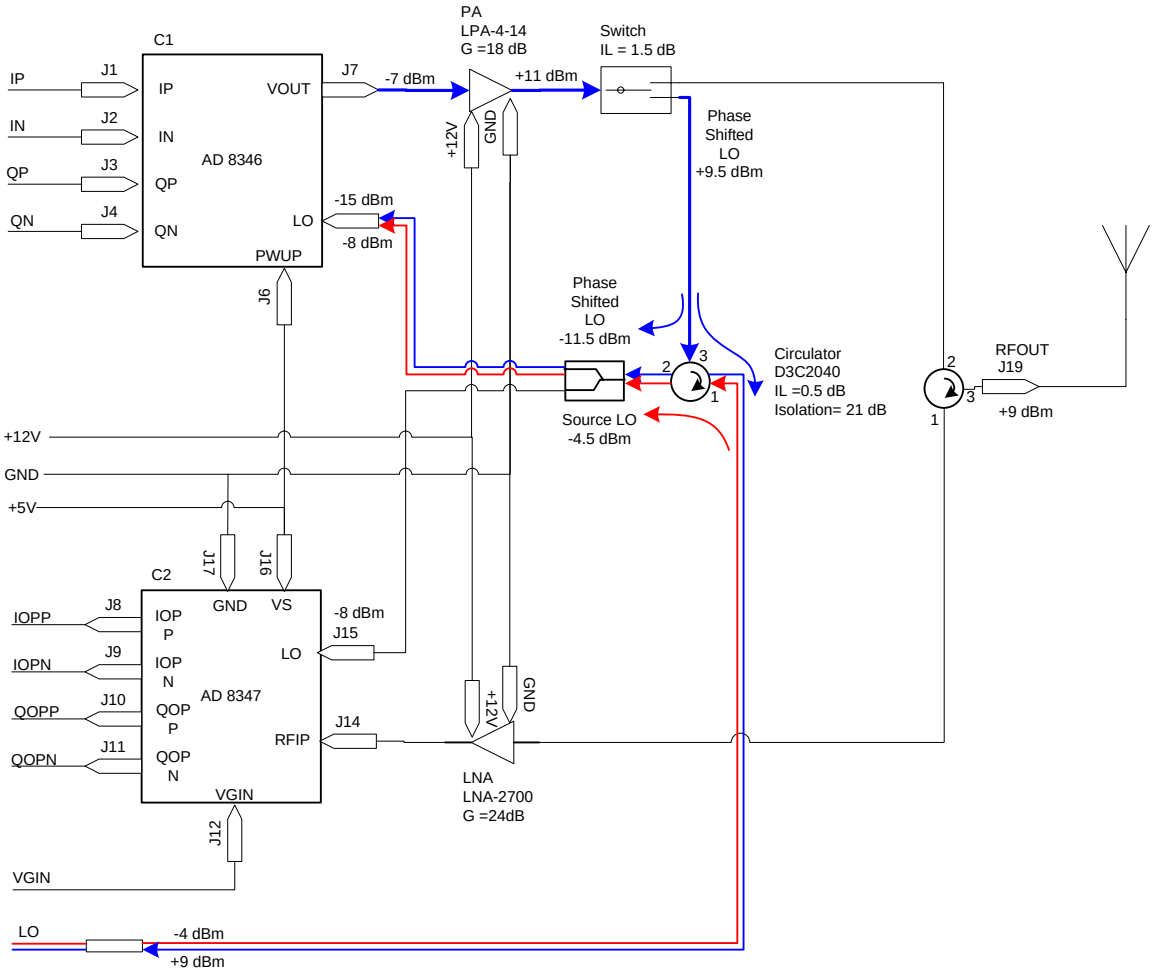

Figure 58. Schematic of T/R module showing power levels at various points in the circuit (After [11]).

C. TRANSMISSION AND RECEPTION BETWEEN T/R MODULES

In order to demonstrate communication between the modules, setup E was used with the antenna elements removed and the RF ports of the two modules connected. Attenuation was added to simulate free space path loss. To verify coherent operation, a

phase shift was introduced in the transmitted signal from module 1 and measured on reception in module 2. The phase was changed over 360 degrees and the received phase plotted vs. transmitted phase (see Figure 59). Errors as large as 60 degrees occurred.

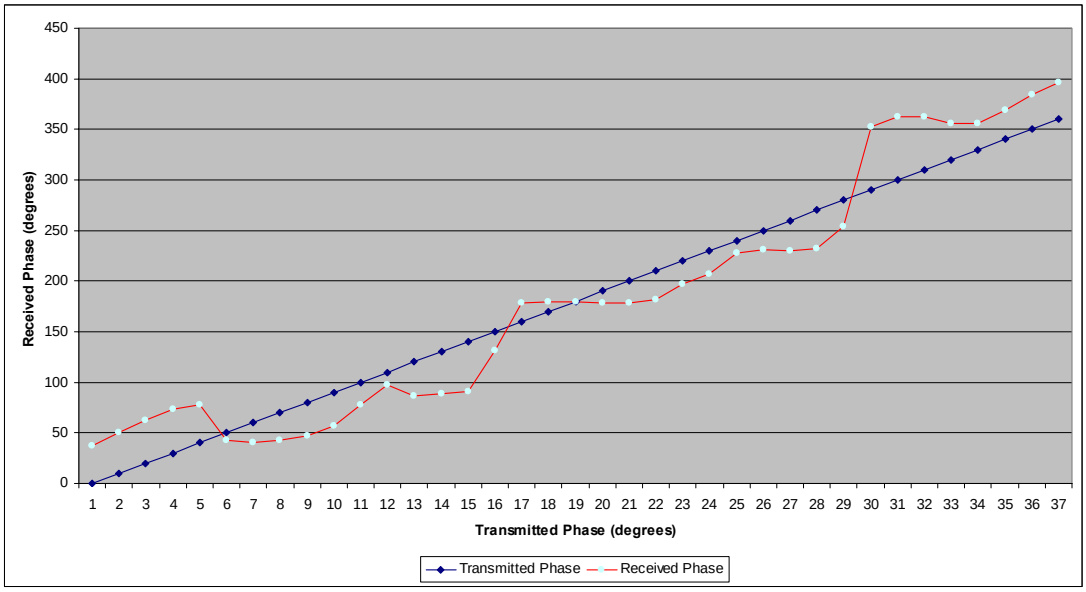

Figure 59. Plot of received phase vs. transmitted phase.

To examine what was causing the large phase errors a series of measurements were conducted. There are three major devices in the transmission chain, and each one of them could be the possible cause of the large phase error: the PA, the low noise amplifier (LNA) or the circulator. In order to determine which one is causing the large phase error we need to verify that the modulator and demodulator are working properly. The first step was therefore to connect the modulator output in the transmitting module 1 directly to the demodulator input in the receiving module 2.

By doing this all devices between the transmitter and receiver were bypassed and performance of the modulator and demodulator could be verified using direct transmission. The result from the direct transmission showed a maximum phase error of 7 degrees as seen in Figure 60.

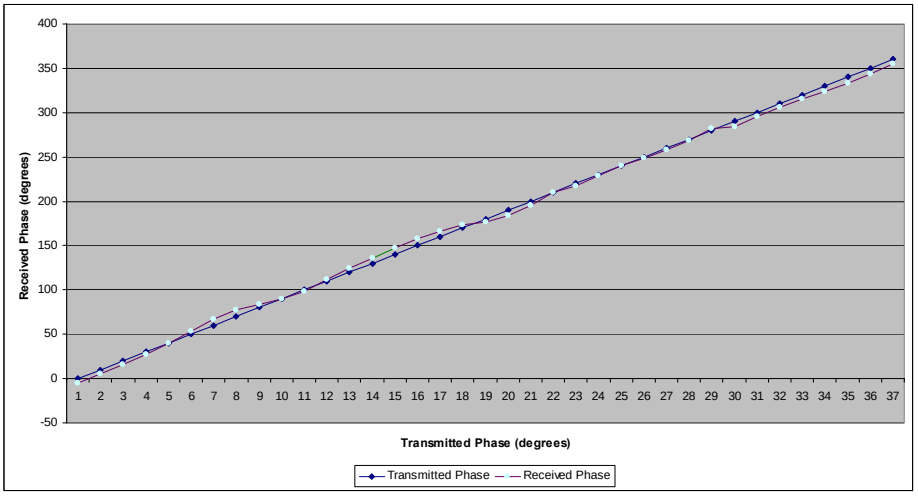

Figure 60. Plot of received phase vs. transmitted phase using a direct connection.

The next step was to bring one device at a time into the transmission chain and do measurements with each new device. This was done so that every device's error contribution in the transmission chain could be measured. The first was the PA, then the LNA, then the PA together with the LNA, and finally all three devices. The results from the measurements are plotted in Figure 61.

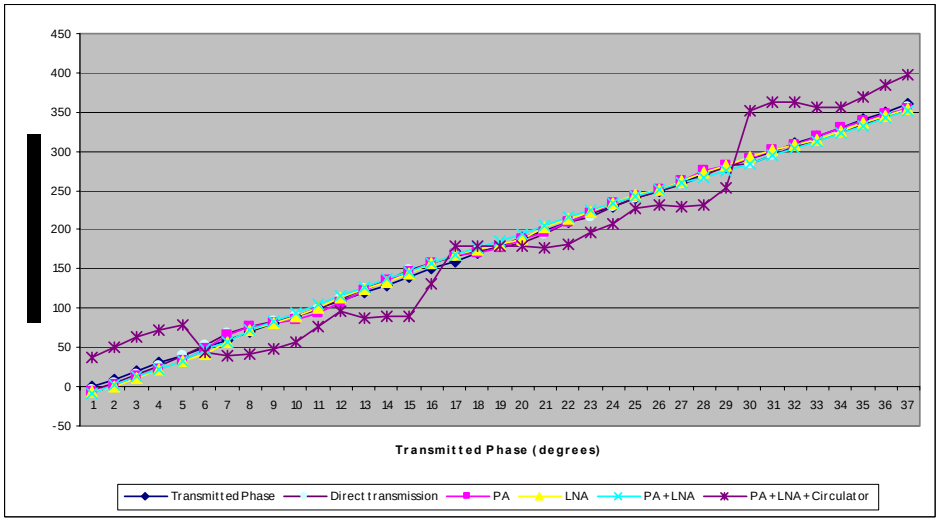

Figure 61. Plot of received phase vs. transmitted phase with different devices in the transmission chain.

It is clear that the circulator is causing the largest contribution to the phase error. A closer look at the affect on the phase error for each device is plotted in Figure 62.

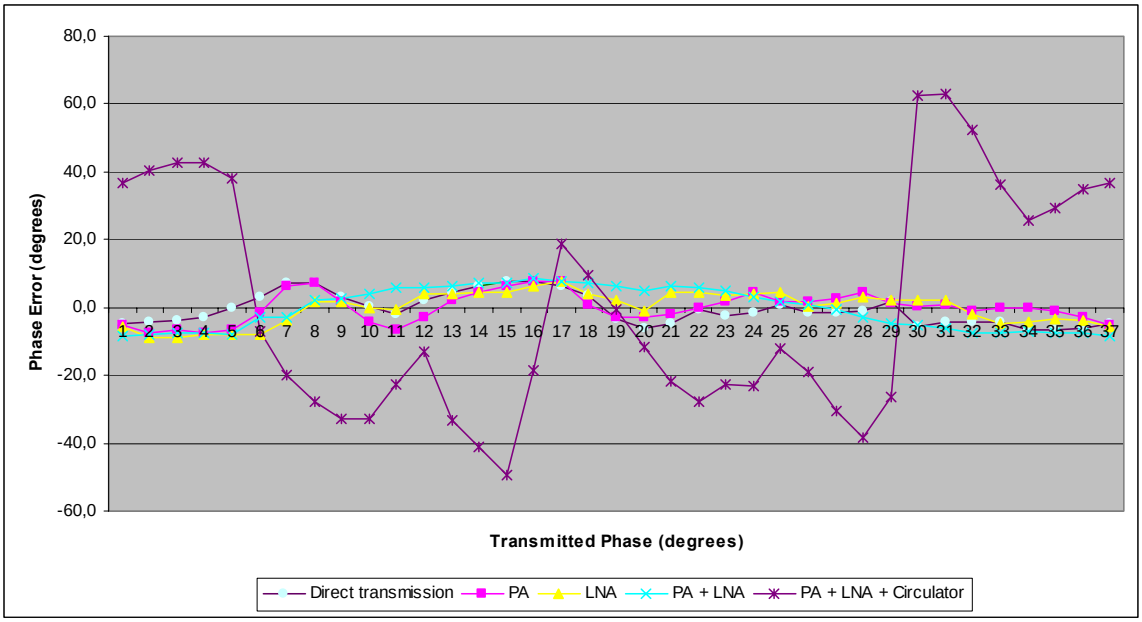

Figure 62. Phase errors between transmitted and received phases.

The device that needs further examination is the circulator. We need to determine why it is causing this large phase error. If it is the circulator, a leakage between the transmit side port and the receive side port, could cause problem (i.e., signal from the modulator could leak to the module's own demodulator). The purpose of a circulator is to isolate the transmit side from the receive side when a single antenna is used. The circulators in the modules have a measured isolation of 21 dB between port 2 and port 1, as seen previously in Figure 38. If we do a power budget for the different signals arriving at the demodulator input we can determine if that isolation is high enough. First we need to measure the signal power level from the modulator arriving at port 2 on the circulator. The power level at the circulator's port 2 was measured under four different operating conditions for the modulator and PA in the receiving module 2 as seen in Table 4. "On vs. Off" in the Tables refers to if power is provided for the PA and the modulator. For all

operating conditions there is zero voltage to the I and Q inputs on the modulator board at the receiving module 2.

Operating Condition		Power level measured at the circulator's port 2
Modulator	PA	
Off	Off	-70 dBm
On	Off	-56 dBm
Off	On	-45 dBm
On	On	-24 dBm

Table 4. Signal power level at circulator port 2, for different operating conditions.

The power levels from Table 4 are then used in a power budget to determine the signal level at the demodulator input under different conditions. The computed values can be seen in Table 5 and it is obvious that the LO feedthrough signal from the receiving module 2 modulator is, under certain conditions, strong enough to cause a large phase error. The operating condition used in Figure 63 was "On/On", where the signal from the module 2 modulator was 7 dB stronger than the received signal from the transmit module 1. However, the "On/On" case is not encountered in radar, because the transmitter will be off while the module is receiving.

Operating Condition		Power level measured at demodulator input, signal coming from	
Modulator	PA	Modulator	RF Antenna
Off	Off	-67 dBm	-28 dBm
On	Off	-53 dBm	-28 dBm
Off	On	-42 dBm	-28 dBm
On	On	-21 dBm	-28 dBm

Table 5. Signal power level at demodulator input, for different operating conditions.

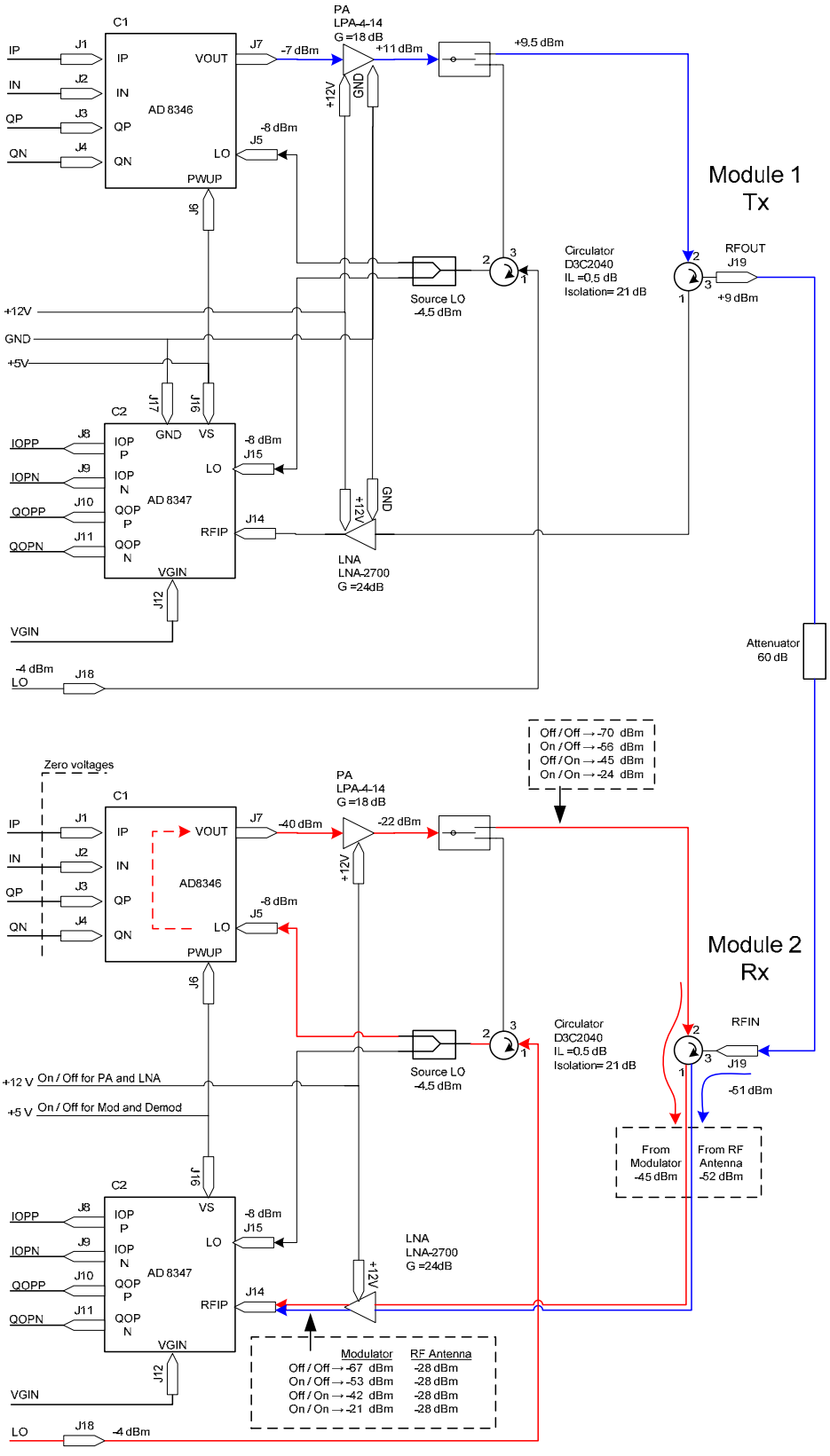

Figure 63. Schematic of transmission from module 1 to module 2.

The LO feedthrough signal comes from the modulator. This signal is present in the modulator output even if the voltage levels on the I and Q inputs are zero. Previous research [31] has shown that there is a LO feedthrough signal present at the modulator output when LO signal is fed to the board.

It is clear that the LO feedthrough signal in combination with leakage in the circulator is causing the large phase error. If we take a closer look at the other devices' contribution, we can see in Figure 64 that they were approximately 7 degrees.

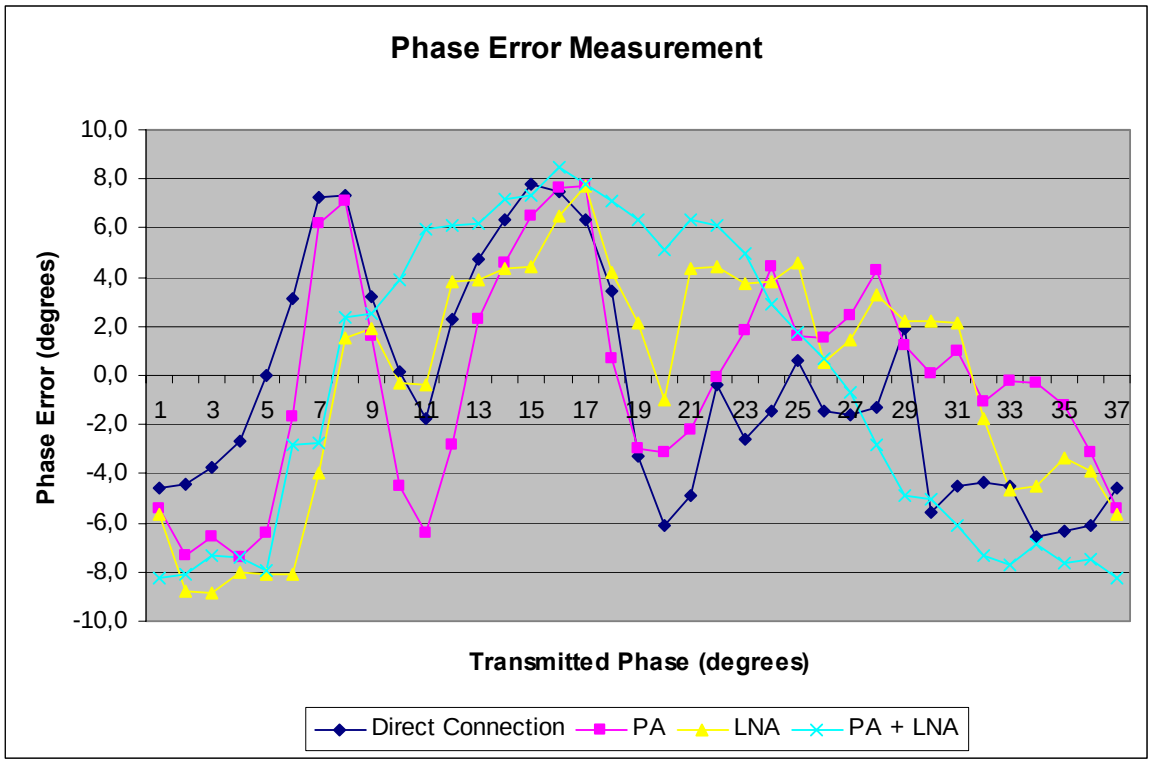

Figure 64. Phase errors between transmitted and received phases.

D. SUMMARY

The phase synchronization circuit was incorporated into the existing T/R modules and they were synchronized using a wireless LO source. It was found that a large phase error was caused by LO feedthrough from the modulator between port 1 and port 2 in the

circulator. The problem can be solved by changing the circulator to one with higher isolation. Previous research has discussed the isolation problem [10] and this thesis verifies it. This is something that needs to be considered in future research.

In conclusion, a phase synchronization circuit was successfully implemented in each of the two T/R modules and a wireless demonstrator test bench was completed as seen in Figure 65.

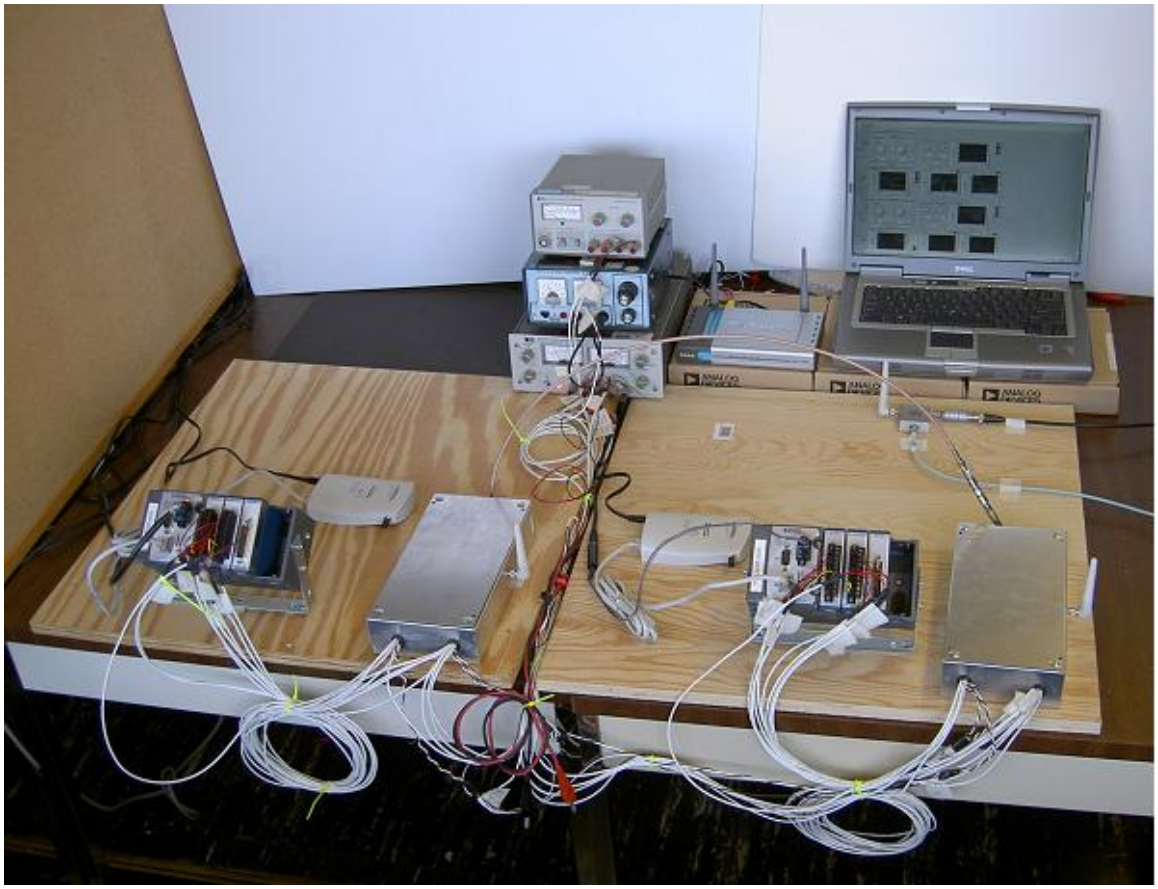

Figure 65. 2-element array wireless demonstration test bench.

VI. CONCLUSIONS AND RECOMMENDATIONS

A. CONCLUSIONS

The focus of this thesis has been on designing a phase synchronization concept, implementing it in existing T/R modules, using Commercial of the Shelf (COTS) hardware, and performing validation measurements of the proposed phase synchronization process. Synchronization circuits where implemented into two Transmit/Receive (T/R) modules and measurements to characterize the new hardware and its performance were done. The results showed that phase synchronization and distribution of LO over the free space channel are possible using the proposed concept.

The concept was validated through a number of measurements where the different parts required for the synchronization circuit have been characterized and verified before being implemented into the T/R modules. The extra circulator and switch were put into the existing T/R modules, and new cables where made for the new hardware. Before attempting the full demonstration of wireless phase synchronization, a wired setup was used to verify the new hardware installation. Instead of the free space channel for LO distribution, cables where used to connect the 2.4 GHz reference signal to the T/R modules. The measurements where done with two different cable lengths connecting the T/R module being synchronized. The theoretical calculation of phase difference due to different cable lengths was verified by measurements and the results showed that the concept was ready for a wireless setup.

The wireless demonstration setup uses 5.8 GHz for the data communication and 2.4 GHz for LO and phase synchronization. The different frequency bands were chosen to minimize interference, and indeed there was no observable interference between them. A number of phase synchronization tests were done with different positions of the LO antenna, symbolizing different T/R module positions, and the measurements verified the concept.

The measurements were not without problems. When changing the position of the power amplifier to include it in the sync circuit, it was discovered that the phase shifted

LO signal was leaking from port 3 to port 2 in the circulator. The circulator was also causing problems in the normal mode where the measured isolation of 21 dB was not enough and LO feedthrough signal was leaking into the demodulator resulting in phase errors as large as 60 degrees. When the two T/R modules were measured in normal mode without the circulators, the agreement was good between the transmitted and received phases.

In conclusion, a phase synchronization circuit was successfully implemented in each of the two T/R modules and a wireless demonstrator test bench was completed. Further design improvements to reduce the impact of the LO feedthrough signal at the demodulator input is necessary though.

B. RECOMMENDATIONS FOR FUTURE WORK

To continue the work to build the prototype eight-element array radar, the following areas need to be addressed:

1. Phase Synchronization

Continue the work on a fully implemented phase synchronization concept, which requires completion of the following tasks:

i. A script in the Controller software that handles the synchronization process.

ii. A connection between the Controller software script and the voltage level output from the detector unit.

2. RF Leakage Cancellation

The circulator's measured isolation of 21 dB is not enough to separate transmit LO feedthrough. It may be possible to due a "coherent subtraction" to cancel the leakage signal.

3. LO Feedthrough Reduction AD8346

The LO feedthrough signal power level from the modulator is affecting the performance. This signal is present in the modulator output even if the voltage levels on I and Q inputs are zero. Previous research [31] has shown that there is a LO feedthrough signal present at the output when LO signal is fed to the board. A design change, or change of modulator, to reduce the LO feedthrough signal power level when the modulator is not in transmit mode, needs further research.

4. Expand the Array Demonstrator

To build an 8-element array, six more T/R modules need to be assembled and tested. For the test and control software, six similar transmit and receive subroutines need to be added to the host VI (*Two Element Array (Host).vi*) and the FPGA VI (*Two Element Array (FPGA).vi*) [11].

THIS PAGE INTENTIONALLY LEFT BLANK

LIST OF REFERENCES

[1] Missile Defense Agency (MDA), "Ballistic Missile Defense System Overview," http://www.mda.mil/mdalink/html/mdalink.html, last retrieved August 2007.

[2] From Wikipedia, the free encyclopedia, "Cobra Dane," http://en.wikipedia.org/wiki/Cobra_Dane, last retrieved August 2007.

[3] Global Security US Weapon Systems (globalsecurity.org), "AN/SPY-1 Radar," http://www.globalsecurity.org/military/systems/ship/systems/an-spy-1.htm, last retrieved August 2007.

[4] Unofficial US Navy site (navybuddies.com), "Aegis Combat System," http://www.navybuddies.com/weapons/aegis.htm#gallery, last retrieved August 2007.

[5] Global Security US Weapon Systems (globalsecurity.org), "Volume Search Radar," http://www.globalsecurity.org/military/systems/ship/systems/vsr.htm, last retrieved August 2007.

[6] Global Security US Weapon Systems (globalsecurity.org), "DDG-1000 Zumwalt," http://www.globalsecurity.org/military/systems/ship/dd-x-specs.htm, last retrieved August 2007.

[7] C. H. Tong, "System study and design of broad-band U-slot microstrip patch antennas for aperstuctures and opportunistic arrays," Master's Thesis, Naval Postgraduate School, Monterey, California, December 2005.

[8] Y. C. Yong, "Receive channel architecture and transmission system for digital array radar," Master's Thesis, Naval Postgraduate School, Monterey, California, December 2005.

[9] Y. Loke, "Sensor synchronization, geolocation and wireless communication in a shipboard opportunistic array," Master's Thesis, Naval Postgraduate School, Monterey, California, March 2006.

[10] G. Burgstaller, "Wirelessly networked opportunistic digital phased array: design and analysis of a 2.4 GHz demonstrator," Master's Thesis, Naval Postgraduate School, Monterey, California, September 2006.

[11] E. C. Yeo, "Wirelessly networked opportunistic digital phased array: system analysis and development of a 2.4 GHz demonstrator," Master's Thesis, Naval Postgraduate School, Monterey, California, December 2006.

[12] D. C. Jenn, Program review, "Wirelessly networked Aperstructure Digital Phased Array," Naval Postgraduate School, May 2007 (unpublished).

[13] S. Gomez, "Wirelessly networked opportunistic digital phased array: system analysis and development of a 2.4 GHz demonstrator," Master's Thesis, Naval Postgraduate School, Monterey, California, September 2007.

[14] National Instruments (ni.com), Data Sheet, "CompactRIO – Real-Time Embedded Controllers, NI cRIO–900x," http://www.ni.com/pdf/products/us/6358_crio_rt_controllers.pdf, last retrieved in August 2007.

[15] National Instruments (ni.com), Data Sheet, "CompactRIO Reconfigurable Chassis, NI cRIO–910x," http://www.ni.com/pdf/products/us/cat_crio_9104.pdf, last retrieved in August 2007.

[16] National Instruments (ni.com), Data Sheet, "C Series Analog Output Modules, NI–9263," http://www.ni.com/pdf/products/us/c_series_ao.pdf, last retrieved in August 2007.

[17] National Instruments (ni.com), Data Sheet, "C Series Analog Input Modules, NI–921x," http://www.ni.com/pdf/products/us/c_series_ai.pdf, last retrieved in August 2007.

[18] Analog Devices (analog.com), Data Sheet, "AD8346 - 2.5 GHz Direct Conversion Quadrature Modulator," http://www.analog.com/en/prod/0%2C2877%2CAD8346%2C00.html, last retrieved in August 2007.

[19] Analog Devices (analog.com), Data Sheet revision A, "AD8346 0.8 GHz to 2.5 GHz Quadrature Modulator," http://www.analog.com/UploadedFiles/Data_Sheets/240325465AD8346_a.pdf, last retrieved in August 2007.

[20] Analog Devices (analog.com), Data Sheet, "AD8346 Evaluation Board," http://www.analog.com/UploadedFiles/Evaluation_Boards/Tools/223525842AD8346EB.pdf, last retrieved in August 2007.

[21] Analog Devices (analog.com), Data Sheet, "AD8347 0.8 GHz to 2.7 GHz Direct Conversion Quadrature Demodulator," http://www.analog.com/UploadedFiles/Data_Sheets/230407246AD8347_a.pdf, last retrieved in August 2007.

[22] Analog Devices (analog.com), Data Sheet, "AD8347 Evaluation Board," http://www.analog.com/UploadedFiles/Evaluation_Boards/Tools/471840006AD8347EB_0.pdf, last retrieved in August 2007.

[23] Filtronic plc (filtronic.co.uk), Data Sheet, "Phase Shifter DC to 2, 4 and 8 GHz, Coaxial," http://www.filtronic.co.uk/pdf/phase_shifters/6X08.pdf, last retrieved in August 2007.

[24] Agilent Technologies (home.agilent.com), 8510C Vector Network Analyser," http://www.home.agilent.com/agilent/product.jspx?nid=-536902671.536879946.00&cc=US&lc=eng , last retrieved in August 2007.

[25] DiTom Microwave Inc. (ditom.com), Data Sheet, "D3C2040 2.00 – 4.00 GHz SMA–Female Circulator," http://www.ditom.com/images/D3C2040.pdf?osCsid=969c6706edd78fde7250d0fea4033987, last retrieved in August 2007.

[26] Mini-Circuits. (minicircuits.com), Data Sheet, "ZASWA-2-50DR High Isolation Switch," http://www.minicircuits.com/pdfs/ZASWA-2-50DR.pdf , last retrieved in August 2007.

[27] D-Link. (dlink.com), Data Sheet, "DWL-7200AP Tri-Mode Dualband Access Point," ftp://ftp10.dlink.com/pdfs/products/DWL-7200AP/DWL-7200AP_ds.pdf , last retrieved in August 2007.

[28] 3COM. (3com.com), Data Sheet, "3Com Wireless LAN Workgroup Bridge," http://www.3com.com/other/pdfs/products/en_US/400856.pdf , last retrieved in August 2007.

[29] National Instruments (ni.com), "NI 9401 8ch, 5V/TTL Digital I/O Module," http://www.ni.com/pdf/products/us/c_series_do.pdf , last retrieved in August 2007.

[30] Anritsu (us.anritsu.com), "RF Detector 75A50 10 MHz to 18.5 GHz," http://www.us.anritsu.com/downloads/files/10100-00010L.pdf , last retrieved in September 2007.

[31] W. Ong, "Commercial off the shelf direct digital synthesizers for digital array radar," Master's Thesis, Naval Postgraduate School, Monterey, California, December 2005.

THIS PAGE INTENTIONALLY LEFT BLANK

INITIAL DISTRIBUTION LIST

1. Defense Technical Information Center
   Ft. Belvoir, Virginia

2. Dudley Knox Library
   Naval Postgraduate School
   Monterey, California

3. Dan C. Boger
   Chairman, Information Sciences Department
   Naval Postgraduate School
   Monterey, California

4. Mr. James King
   Naval Surface Warfare Center
   Carderock Division
   West Betheseda, Maryland

5. Mr. Steven Russell
   Office of Naval Research
   Arlington, Virginia

6. Prof. David Jenn
   Department of Electrical & Computer Engineering
   Naval Postgraduate School
   Monterey, California

7. Robert Broadston
   Department of Electrical & Computer Engineering
   Naval Postgraduate School
   Monterey, California

8. Nicholas Willis
   Consultant
   Carmel, California

9. William Solitario
   Northrop Grumman Ship Systems
   Naval Postgraduate School
   Monterey, California

10. Prof. Michael Melich
Wayne E. Meyer Institute of System Engineering
Naval Postgraduate School
Monterey, California

11. Siew Yam Yeo
Ag AD (SV)
DRD/DSTA
Singapore